

SEISMIC RECORD OF LATE OLIGOCENE THROUGH MIocene GLACIATION ON THE CENTRAL AND EASTERN CONTINENTAL SHELF OF THE ROSS SEA

Laura De Santis¹

Universita' di Parma, Parma, Italy

John B. Anderson

Department of Geology and Geophysics, Rice University, Houston, Texas

Giuliano Brancolini

Osservatorio Geofisico Sperimentale, Trieste, Italy

Igor Zayatz

Joint Stock Company Marine Arctic Geological Expedition, Murmansk, Russia

INTRODUCTION

The geological record of ice sheet development on Antarctica must be extracted, in large part, from offshore strata because the continent is 98% ice-covered. The ice sheet has been the focus of numerous studies since the first sediment cores and seismic data were collected from the Antarctic sea floor three decades ago. However the marine record has yielded contradictory results, particularly the deep-sea proxy record (i.e., variations in ice rafted detritus with depth in sediment cores, the stratigraphic occurrence of deep sea hiatuses, and the oxygen isotope record).

The Ross Sea is a key area in which to investigate Antarctic Ice Sheet evolution. It is the terminus for ice covering over 20% of the Antarctic continent, and drill cores have shown that it contains several kilometers of glacial marine Cenozoic strata dating back at least to middle Eocene times [Hayes and Frakes, 1975; Barrett, 1986, 1989; Hannah, 1994]. However, timing of the first advance of ice sheets onto the continental shelf is still unclear, and interpretations of the sedimentary environments are still debated [Hayes and Frakes, 1975; Balshaw, 1981; Leckie and Webb, 1983; Hambrey et al., 1989; Bartek et al., 1992; Jiang and Harwood, 1992; Hambrey and Barrett, 1993].

Seismic reflection data may provide a direct record of ice sheet grounding events, in the forms of glacial erosion surfaces and subglacial and grounding-line proximal seismic facies. Several attempts have been made at examining the Ross Sea's glacial history using seismic data. Houtz and Meijer [1970] and Houtz and Davey [1973] identified a widespread glacial erosion surface on the shelf, "Ross Sea Unconformity", which was later drilled during DSDP Leg 28 and assigned an age of Plio-Pleistocene [Hayes and Frakes, 1975]. Savage and Ciesielski [1983] re-examined microfossils from these sites and argued that the ice sheet first grounded on the continental shelf sometime between 10.3 and 8.8 Ma. Cooper et al. [1991a] proposed a model in which grounded ice sheets are viewed as the principal mechanism for depositing the Cenozoic prograding sequences of the Ross Sea continental margin. In this model, gently dipping glacial strata were deposited during the initial advance of the grounded ice sheet, while trough-mouth fans and sheet-like prograding sequences were deposited when the ice sheet was grounded at the continental shelf edge. They suggested that the ice sheet first reached the continental shelf edge in the early Miocene. This is in general agreement with the results of Anderson and Bartek [1992], who observed glacial features, such as landward dipping erosional surfaces, till tongues, grounding zone wedges and trough mouth fans in the early Miocene sequences on the shelf.

¹Also at Osservatorio Geofisico Sperimentale, Trieste, Italy

Previous seismic stratigraphic studies in the Ross Sea were limited by the type of data used. The single-channel, high- to intermediate-resolution data used by *Anderson and Bartek* [1992] provided a good balance between resolution and depth of penetration, allowing seismic facies analysis of most shallow parts of the glacial section. However these data do not penetrate clearly below the water-bottom-multiple reflection. The multichannel (MCS) data from the Ross Sea lacks the resolution needed for detailed seismic facies analysis, but they image older strata below the water-bottom multiple. Together, the two data sets provide extensive coverage of the Ross Sea continental shelf. This paper presents results of an integrated seismic stratigraphic investigation to reconstruct the Oligocene through Miocene glacial settings in the central and eastern Ross Sea.

METHODS

The data sets used for this study consist of high-, intermediate- and low-resolution seismic reflection data (Figure 1, Table 1) and published lithologic and

biostratigraphic descriptions from DSDP Leg 28 drill sites [*Hayes and Frakes*, 1975; *Balshaw*, 1981; *Leckie and Webb*, 1983; *Jiang and Harwood*, 1992; *Hambrey and Barrett*, 1993].

By integrating the different types of seismic reflection records, we were able to resolve and map the varied seismic facies that we interpreted as subglacial, ice-proximal and ice-distal glaciomarine deposits, based on examples from other glaciated areas [*King and Fader*, 1986; *King et al.*, 1991; *Belknap et al.*, 1989; *Shipp et al.*, 1989; *Vorren et al.*, 1990; *Stocker*, 1990; *Belknap and Shipp*, 1991; *Saettem et al.*, 1992; *King*, 1993; *Syvitski*, 1991], and from the Ross Sea [*Anderson and Bartek*, 1992]. Glacial features on seismic data at different resolutions are shown in Figures 2a and 2b.

Several seismic unconformities, previously recognized by *Hinz and Block* [1984] and *Cooper et al.* [1991a], were described and mapped in the Ross Sea by the ANTOSTRAT (Antarctic Offshore Acoustic Stratigraphy) project using MCS data [*Busetti and Zayatz*, 1994; *Brancolini et al.*, this volume(a)]. Maps of these unconformities are shown in ANTOSTRAT [this volume, Plates 16-19]. The ages of the Ross Sea unconformities (RSU6 to RSU1) range from Eocene-Oligocene(?) to late Pleistocene, based on correlation with DSDP Leg 28 drill sites (Table 2). Our study focused on a seismic facies analysis of Ross Sea

TABLE 1. Seismic Data

Seismic source (liter)	Vertical resolution (meters)	Penetration depth (seconds)	Scientific institution and year	Seismic survey (km)
Sparker 100J	5-7	0.2	MAGE ¹ 1989	3,100
Air gun 2.46	12	1.5-2.0	Rice ² 1990	2,600
Air gun 45.16	40	6	OGS ³ 1988, 1989	6,425
Air gun 22.5	20-30	3-4	OGS ³ 1990	2,533
Air gun 10	60-70	6	MAGE ¹ 1987, 1989	7,495
Air gun 23.45	30	6	BGR ⁴ 1980	6,743
Air gun 35.54	30	6	IFP ⁵ 1982	2,000
Air gun 21.3	30	6	USGS ⁶ 1984	1,850
Air gun 9.2	30	6	JNOC ⁷ 1983	1,670

¹Joint Stock Company Marine Arctic Geological Expedition (Russia)

²Rice University (USA)

³Osservatorio Geofisico Sperimentale di Trieste (Italy)

⁴Bundesanstalt für Geowissenschaften und Rohstoffe (Germany)

⁵Institut Français du Pétrole

⁶U. S. Geological Survey

⁷Japanese National Oil Company

TABLE 2. Age and Boundaries for Ross Sea Seismic Sequences (RSS)

Seismic sequence	Sequence boundaries	Age
RSS-8	Sea floor	Plio(?) - Pleistocene
RSS-7	RSU1	Plio(?) - Pleistocene
RSS-6	RSU2	late Miocene and early Pliocene
	RSU3	
RSS-5		middle to late Miocene
	RSU4	
RSS-4		early to middle Miocene
	RSU4A	
RSS-3		early Miocene
	RSU5	
RSS-2		late Oligocene and early Miocene
	RSU6	
RSS-1		Cretaceous(?) to Oligocene(?)
	Basement	

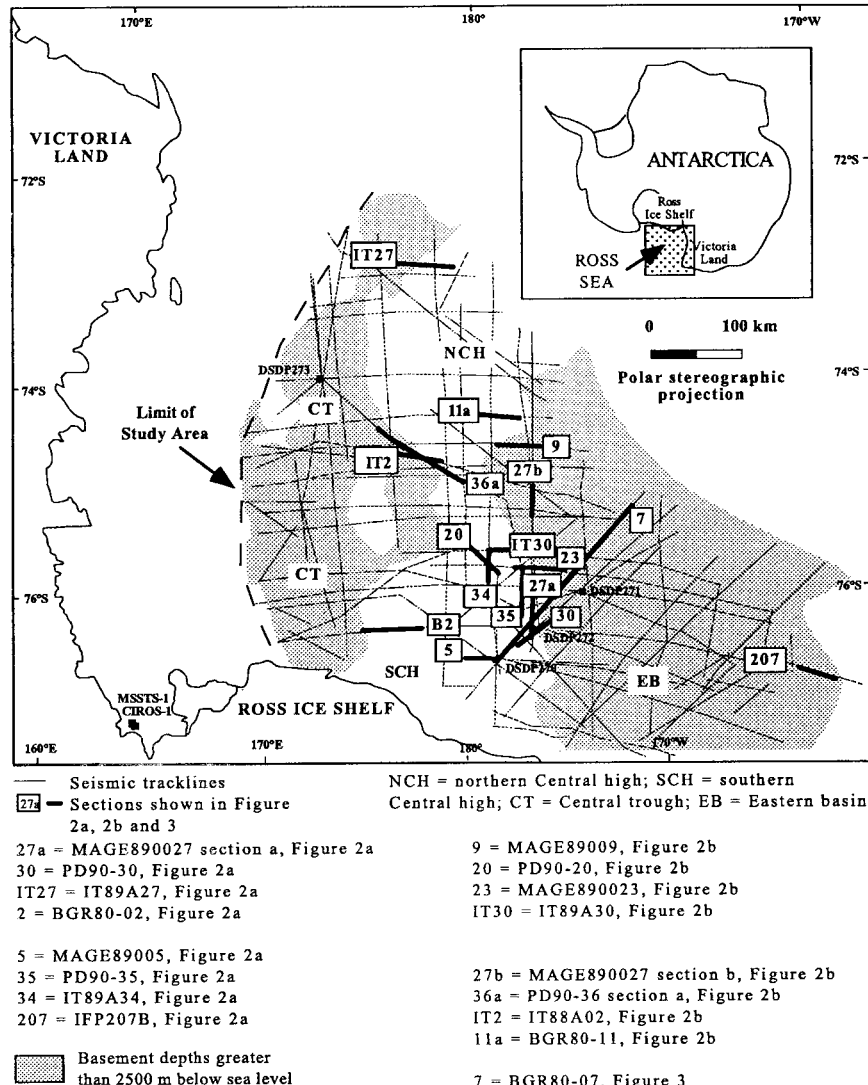


Fig. 1. Location map of the Ross Sea and seismic tracklines of profiles shown in Figures 2 and 3.

sequences 1 to 5 (RSS-1 to RSS-5), which are illustrated in MCS Profile BGR80-07 (Figure 3; see also *ANTOSTRAT*, this volume, Plate 14).

DESCRIPTION OF SEISMIC FACIES AND EROSIONAL FEATURES

3.1. Seismic Facies

We have identified three main acoustic facies in seismic sections from the central and eastern Ross Sea; a non-reflective facies A, a stratified facies B (with occasional non-reflective lenses) and an intermediate facies C.

3.1.1. Facies A. Facies A is composed of partly reflective bodies typically ranging in thickness from 50 to 200 msec and in extent around several kilometers.

The bodies are bounded by oblique-tangential clinoforms dipping at about 1° (Figures 2a and 4), and they downlap onto sub-horizontal reflectors, though some bounding surfaces are concave and plainly erosional.

The facies appears on strike lines (Figure 2a) to be more internally chaotic, with non-reflective lenses bounded by high-amplitude concave reflectors thought to represent large cut and fill structures. On dip lines (Figure 2b), the facies typically has a wedge geometry with downlap onto sub-horizontal reflectors. Around the flanks of basement highs, wedges of facies A are cut by sharp erosion surfaces (Figures 3 and 4) and locally have a bank-like external shape (Figure 5).

The wedges of facies A in sequences RSS-2 and RSS-3 are smaller than in RSS-4, and they have been observed only in a few areas on the flanks of the

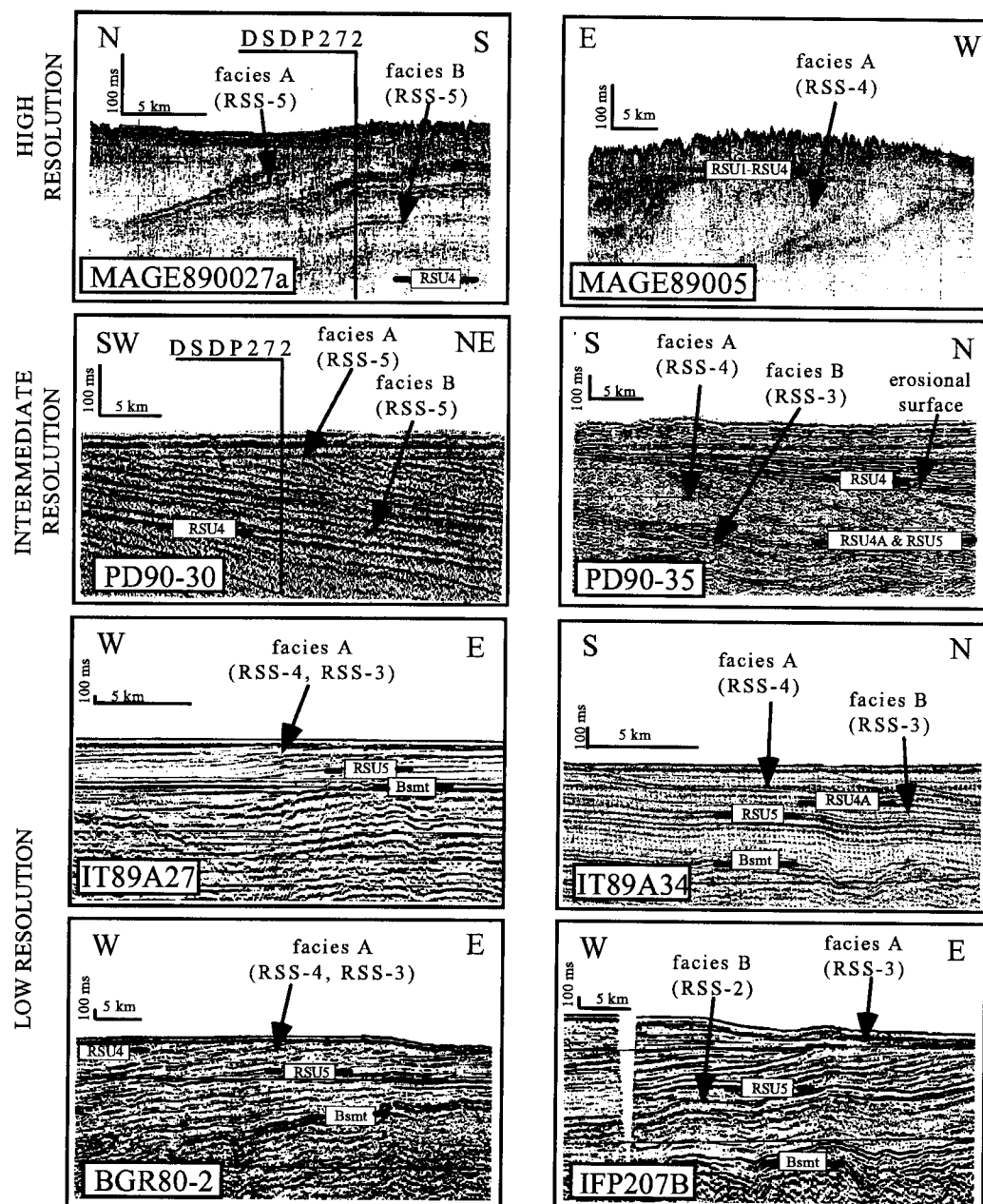


Fig. 2. Examples of seismic facies A and B as imaged in high-, intermediate- and low-resolution seismic reflection profiles. Lower-frequency seismic profiles yield lesser resolution but image deeper units. See Figure 1 for locations.

(a) Dip sections. Facies A is typically non-reflective wedges 200 ms thick bounded by high-amplitude oblique-tangential clinoforms that downlap onto parallel, sub-horizontal reflectors. These are interpreted as ice-proximal deposits. Facies B comprises subparallel, subhorizontal, continuous high-to-medium amplitude reflectors shaped as basin fill. These are interpreted as ice-distal deposits.

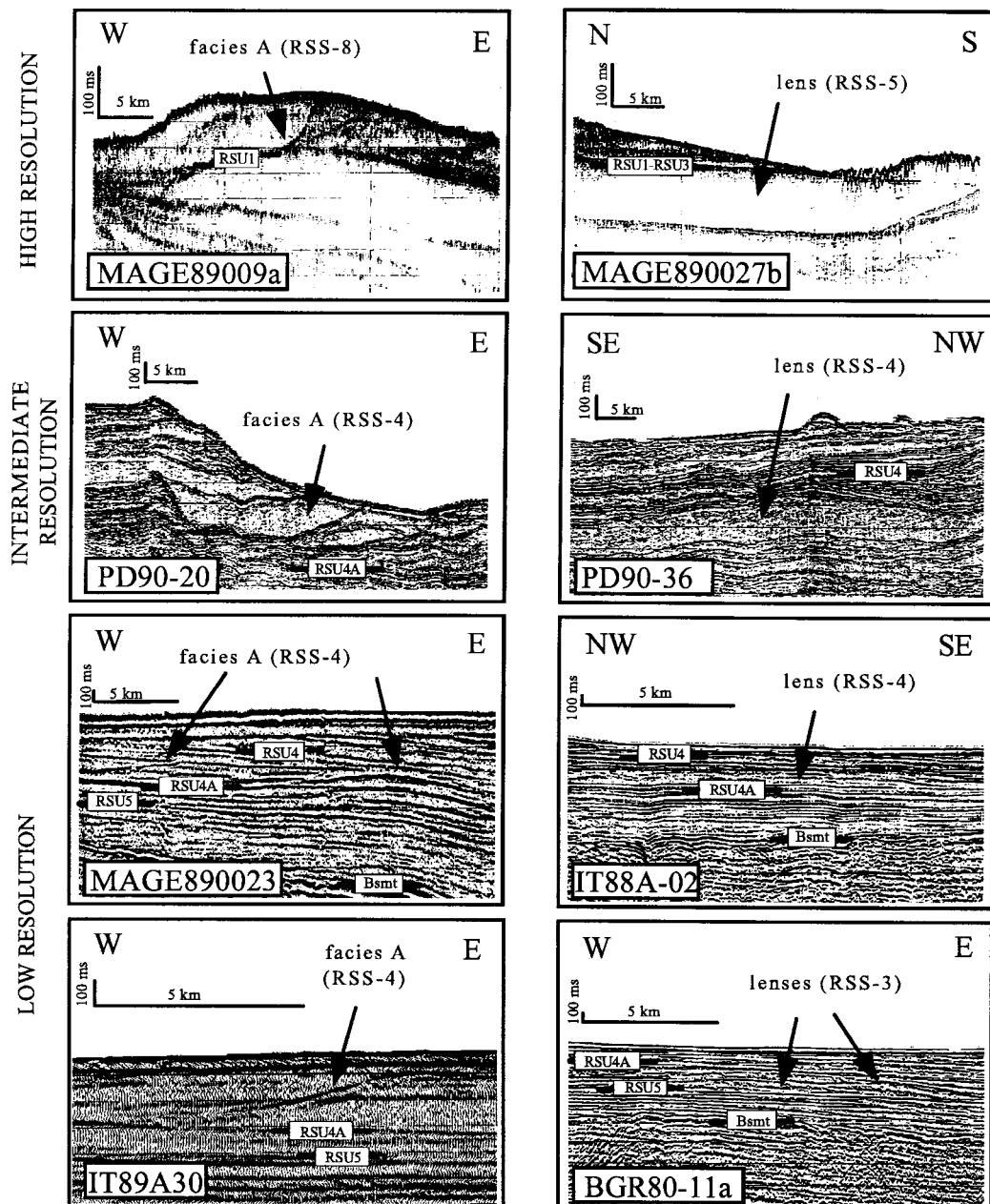


Fig. 2 (cont.). (b) Strike sections. Facies A (left) appears as non-reflective lenses truncated by high amplitude reflectors. Facies B (right) commonly has lenses that occur as single non-reflective bodies interlayered with, and draped by, stratified material. The lenses are interpreted as deposits of slumps or debris flows.

Central high (Figure 6). In contrast, facies A in RSS-4 is composed of large, massive wedges with clinoforms that prograde for several tens of kilometers (Figure 2a). Figures 6 and 7 show these bodies prograding toward the centers of basins from formerly high-standing areas.

3.1.2. Facies B. Facies B is stratified, with high amplitude, continuous, parallel and sub-horizontal reflectors (Figure 2). It typically includes sporadic non-reflective to chaotic lenses several tens of km long and 100-200 msec thick that are convex upwards on strike lines (Figure 2b, line BGR80-11b). The lenses show

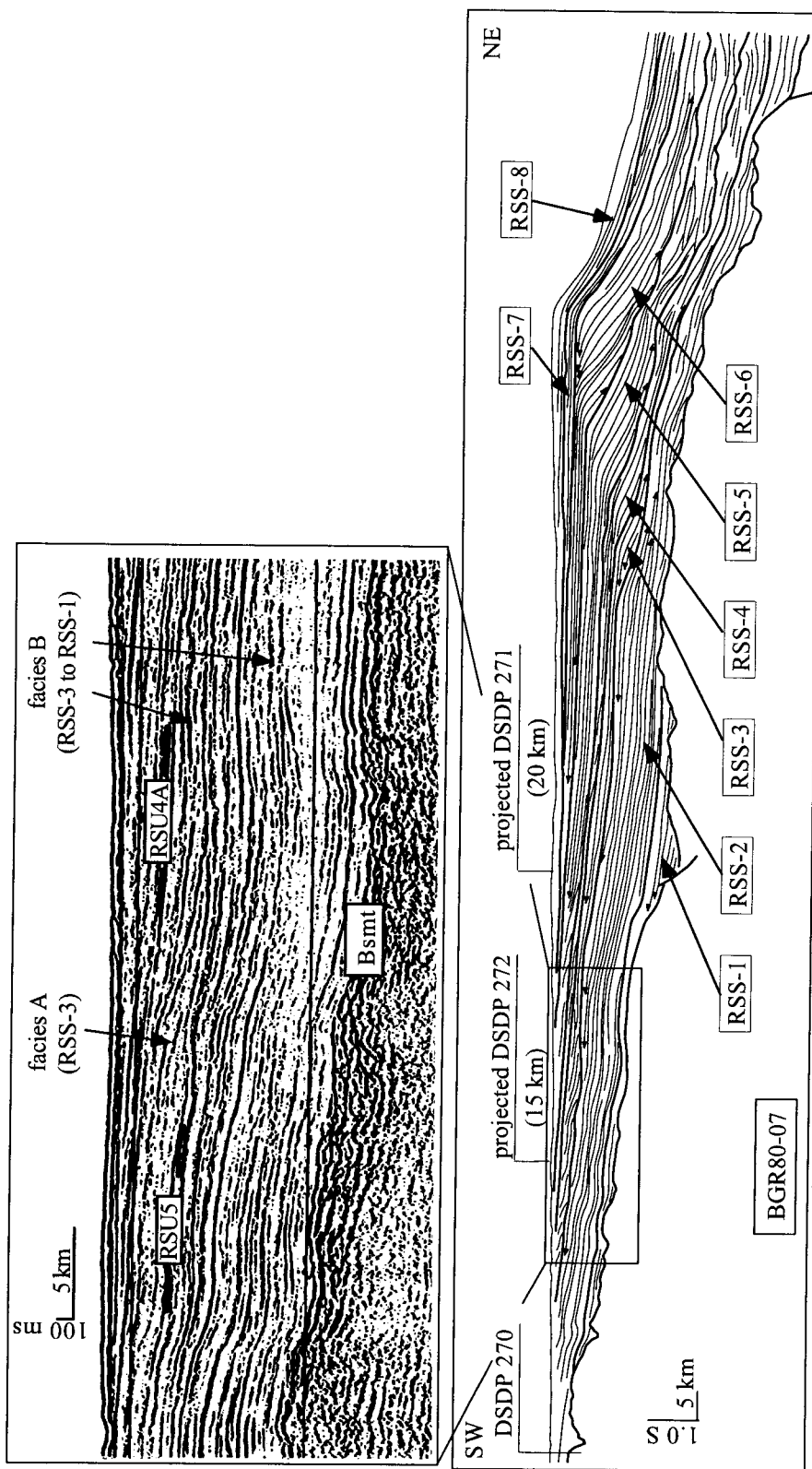


Fig. 3. Seismic profile BGR80-7 illustrates the stratal geometries of sequences described in this paper. Note the increase in foreset dips at the paleo-shelf edge of RSS-2 to RSS-8. See Figures 1 and 6 for the profile location.

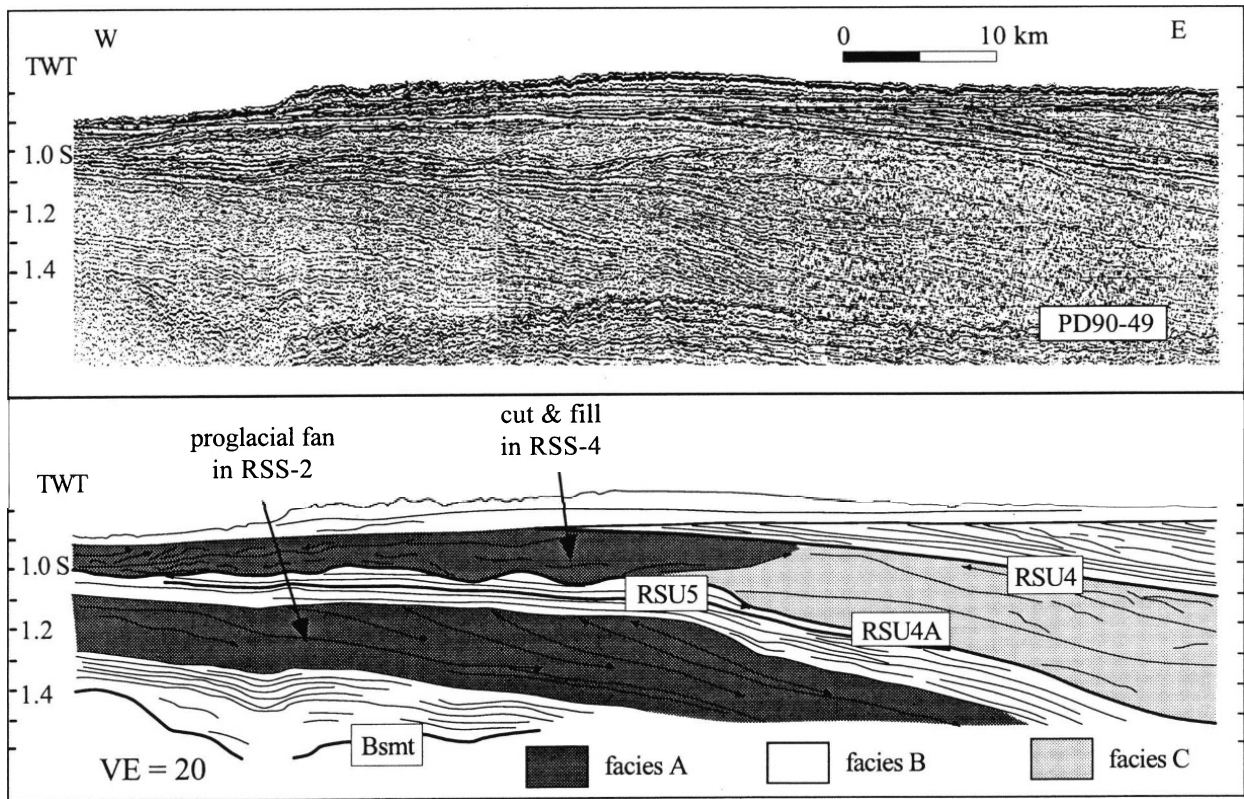


Fig. 4. Segment of seismic profile PD90-49 (intermediate-resolution data) and interpretation. The dark gray pattern highlights a wedge of facies A in RSS-2, and cut-and-fill features of facies A in RSS-4. These are interpreted as proglacial fans. The RSS-2 fan is observed in a down-dip direction and the RSS-4 fan in strike view. Toward the basin (toward the right), along the eastern flank of the Central high, facies A in RSS-4 becomes less massive, and changes to facies C. See Figure 6 for profile location.

irregular upper surfaces and internally show discontinuous, scattered and hummocky reflectors.

Facies B strata onlap the flanks of basement highs, where they commonly interfinger with facies C, and dominate in the surrounding basins.

3.1.3. Facies C. Facies C is intermediate in character between facies A and facies B. It is a mix of internal low-amplitude, and low-angle to sub-horizontal reflectors like facies B with a higher abundance of the partly reflective to chaotic lenses generally less than 100 msec thick and few km long, giving it in places the partly reflective aspect of facies A.

Facies C was deposited on the flanks of structural highs (Figure 7), and is interlayered with non-stratified facies A and stratified facies B (Figures 8 and 9). Toward the basinal areas, facies C becomes more reflective and more stratified (Figure 9).

3.2. Erosional Features

We note erosional features on three scales, ranging from small channels a few kilometers wide through large erosion troughs to regional unconformities, in the central and eastern Ross Sea.

3.2.1. Small channels in basement. U-shaped channels are incised into acoustic basement on structural highs (Figure 10). The channels are around 5 km wide, a few tens of km long, and have a relief of 200–500 msec. The heads of these channels lie topographically above the termination of RSU6 against the basement, but basinward the channels are infilled by RSS-1 and overlain by RSU6 (Figure 10). Structure contour maps (in time) for depth to acoustic basement beneath two sectors of the Central high (Figure 11) show that the U-shaped channels occur around the perimeter of the Central high, ending at the outer

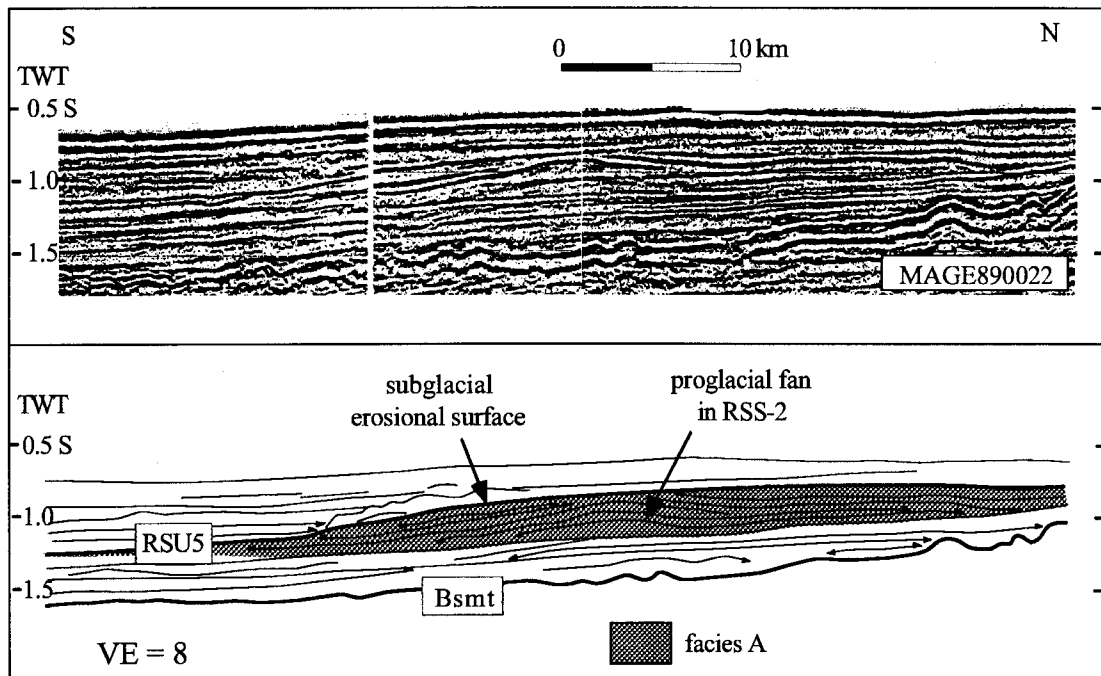


Fig. 5. Segment of seismic profile MAGE890022 (low-resolution data) and interpretation illustrating facies A with a bank-like external shape and southward-dipping foresets that prograde from the Central high. See Figure 6 for profile location.

margin of the basement plateau, where the eroded basement surface steepens.

3.2.2. Large troughs. Large erosional troughs several tens of km wide and with a relief of 200–300 msec are observed in the sedimentary section between the northern and southern parts of the Central high. The troughs are at unconformity RSU4 and locally at RSU5, and are covered by facies B (Figures 12 and 13). In the Eastern basin near the continental paleo-shelf edge, the eastern wall of a similar trough is observed at RSU3 (Figure 14). The relief of the RSU3 trough is comparable with that of troughs carved into the Ross Sea continental shelf by Holocene ice-streams (see "modern glacial trough" in Figure 14).

3.2.3. Regional unconformities. As noted above in the Methods section, regional unconformities (RSU6–RSU1) separate the seismic sequences (RSS-1 to RSS-8). The unconformities are erosion surfaces that are commonly amalgamated and sharply truncate wedges of facies A across the flanks and crests of structural highs. Toward the basins, the unconformities become almost conformable with basin strata of facies B and C. Beneath the outer shelf of the eastern Ross Sea, the unconformities form paleo-shelf-edges and separate

sequences with topset and foreset strata with variable amounts of erosion.

3.3. Seismic Sequences of the Outer Shelf

In the eastern Ross Sea, the seismic sequences near the continental paleo-shelf edges lie in wedges that have topset and foreset strata with variable thicknesses and dips (Figure 3; *ANTOSTRAT*, this volume, Plate 14). Sequence RSS-1 does not have a distinct paleo-shelf edge. Sequences RSS-2 and RSS-3 are characterized by aggradational geometries in the sedimentary wedges near the paleo-shelf edges. In these sequences, the average inclination of foreset beds ranges from less than 2° to 4° . Sequences RSS-4 and RSS-5 become more progradational up section, and the amount of progradation varies along the paleo-shelf edge. Within sequence RSS-6, there is a major seaward shift of the paleo-shelf edge, and foreset beds are sharply truncated (Figure 3). Sequence RSS-7 is characterized by steeper foreset strata than RSS-6, and is cut by sharp erosional surfaces, as previously observed by Cooper *et al.* [1991a], Alonso *et al.* [1992] and Anderson and Bartek [1992]. Further descriptions

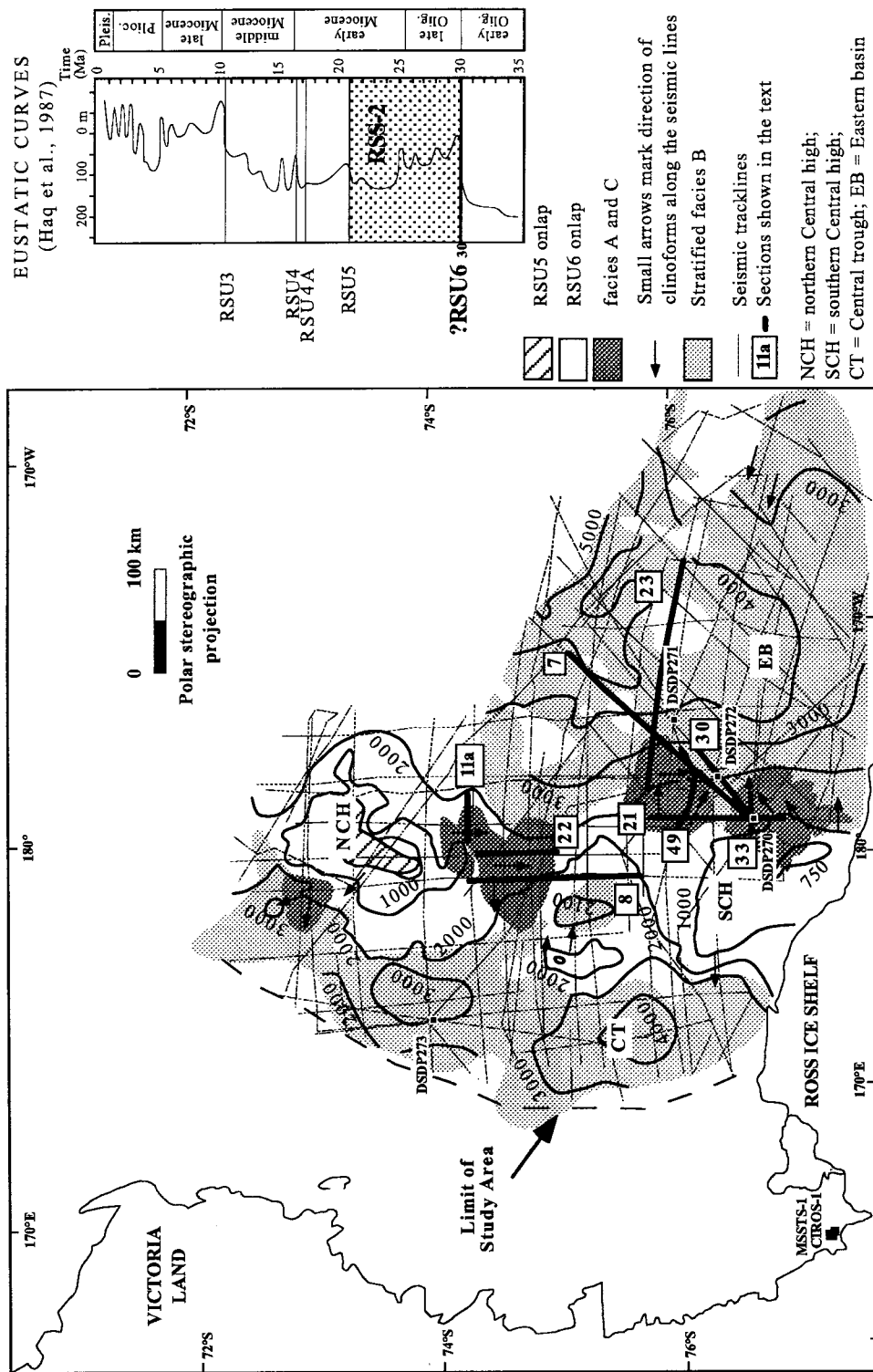


Fig. 6. Structure contour map of RSU6 (depths from sea surface in meters) and distribution of seismic facies in the late Oligocene-early Miocene sequence RS-2. Numbers in squares correspond to the seismic sections shown in this paper: 11a = BGR80-11 section a, Figure 2b; 30 = PD90-30, Figure 9; 7 = BGR80-07, Figure 3; 49 = PD90-49, Figure 4; 22 = MAGEE90022, Figure 5; 21 = PD90-21, Figure 8; 33 = IT89A33, Figure 10; 8 = BGR80-08, Figure 13.

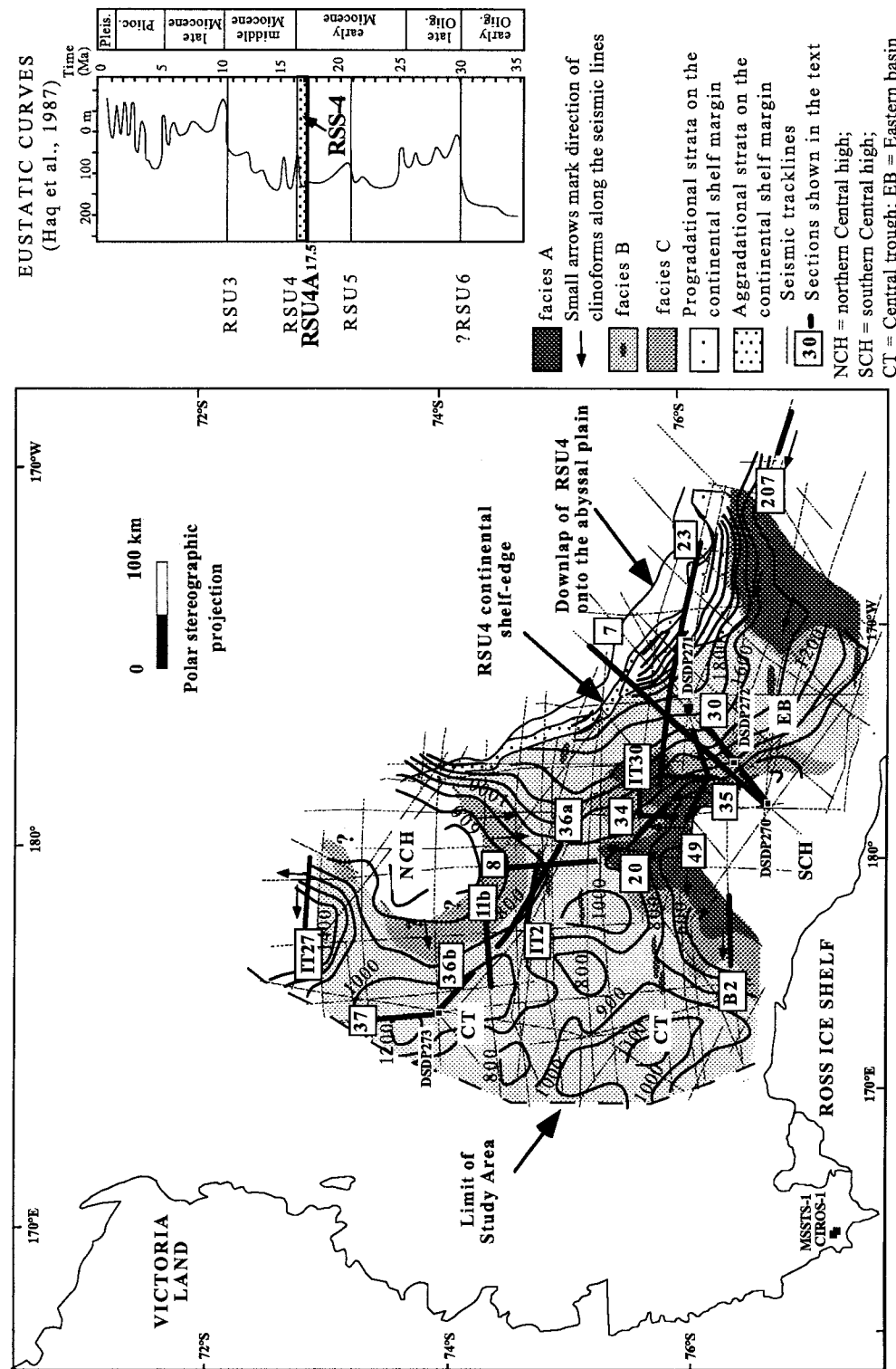


Fig. 7. Structure contour map of RSU4A (depths from sea surface in meters) and distribution of seismic facies in the early to middle Miocene sequence RSS-4. Numbers in squares correspond to the seismic sections shown in this paper: 35 = PD90-35, Figure 2a; 34 = IT89A34, Figure 2a; 207 = IFPB, Figure 2a; IT27 = IT89A27, Figure 2a; 2 = BGR80-02, Figure 2b; IT30 = IT89A30, Figure 2b; IT2 = IT89A02, Figure 2b; 7 = BGR80-07, Figure 3; 49 = PD90-49, Figure 4; 30 = PD90-30, Figure 9; 36a = PD90-36 section a, Figure 12; 11b = BGR80-11 section b, Figure 12; 8 = BGR80-08, Figure 13; 23 = MAGE890023, Figure 14; 36b = PD90-36 section b, Figure 16; 37 = PD90-37, Figure 16.

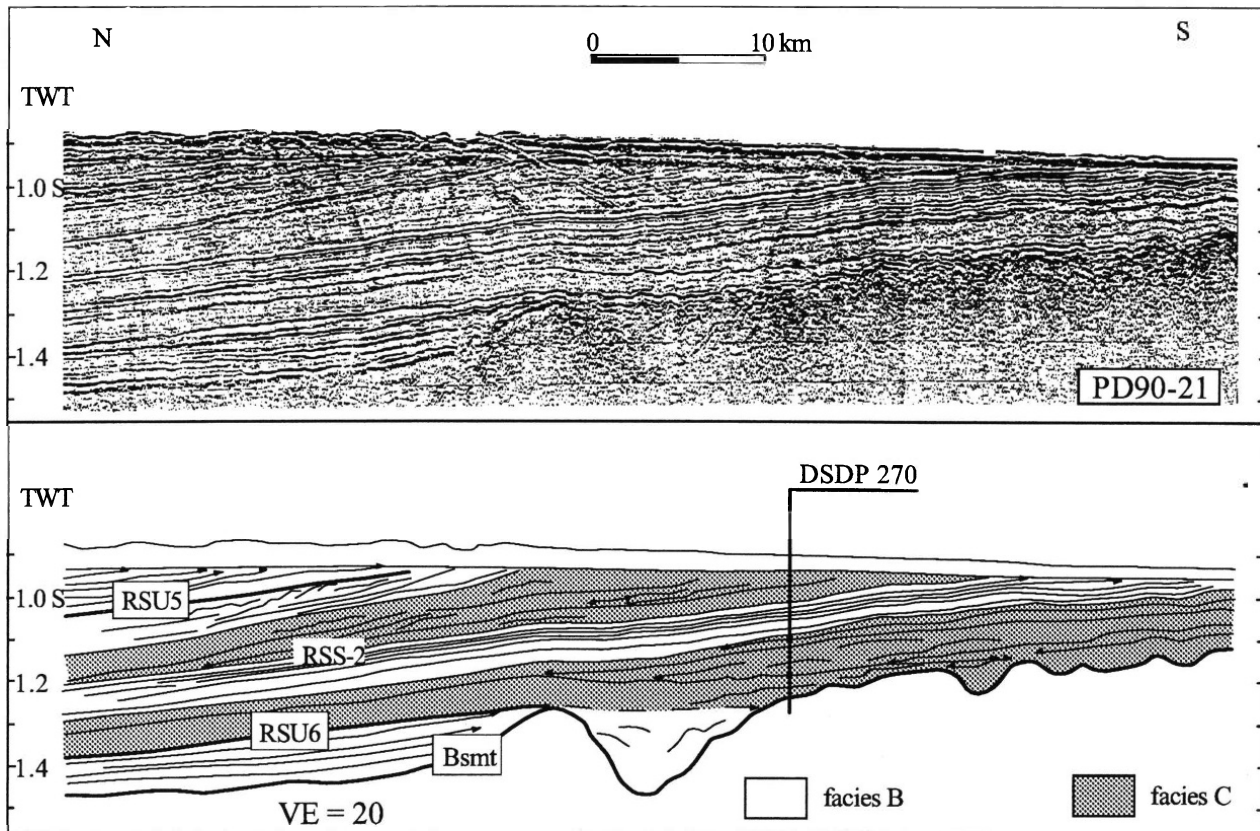


Fig. 8. Segment of seismic profile PD90-21 (intermediate-resolution data) and interpretation. We believe that the vertical alternation of seismic facies between massive (C) and stratified (B) denotes transgressive/regressive cycles related to glacio-eustatic changes. These are superimposed on an overall tectonic subsidence that increased paleo-water depth from 50 to 500 m at DSDP Site 270 during early Miocene time [Leckie and Webb, 1983]. See Figure 6 for profile location.

of the seismic sequences for the central and western Ross Sea are given in Brancolini *et al.* [this volume(b)].

INTERPRETATION OF EROSION FEATURES AND SEISMIC FACIES

4.1. Erosional Features

4.1.1. Small channels in basement. Small U-shaped channels like those incised into acoustic basement on the Central high are commonly associated with glacial erosion, although a fluvial origin cannot be discounted. The size (around 5 km wide, few tens of km long, and 200–500 msec relief) and geometry of these channels are similar to submarine channels described in other glaciated areas, such as the continental shelf of Alaska [Carlson *et al.*, 1982; Armentrout, 1983, 1994].

DSDP Site 270 sampled the flank of a feature that we believe is a glacial channel (Figure 10). The recovery of a soil bed and shallow marine sandstone at the base of DSDP Site 270 [Hayes and Frakes, 1975] indicates that the channel likely formed in subaerial and shallow marine environments.

4.1.2. Large troughs. Anderson and Bartek [1992] observed that unconformity RSU4 displays in places similar relief to bathymetric troughs in the Ross Sea that were carved by ice streams (Figure 12, line PD90-36a). Figure 13 shows a similar feature associated with RSU5. The buried troughs of RSU5 and RSU4 are restricted to the shallower parts of the central continental shelf, and they trend perpendicular to the Central high and to the present bathymetric troughs. We therefore interpret the buried troughs as being carved by local ice caps originating on the Central high. Erosional troughs many tens of km wide and indicating erosion of many hundreds of meters occur

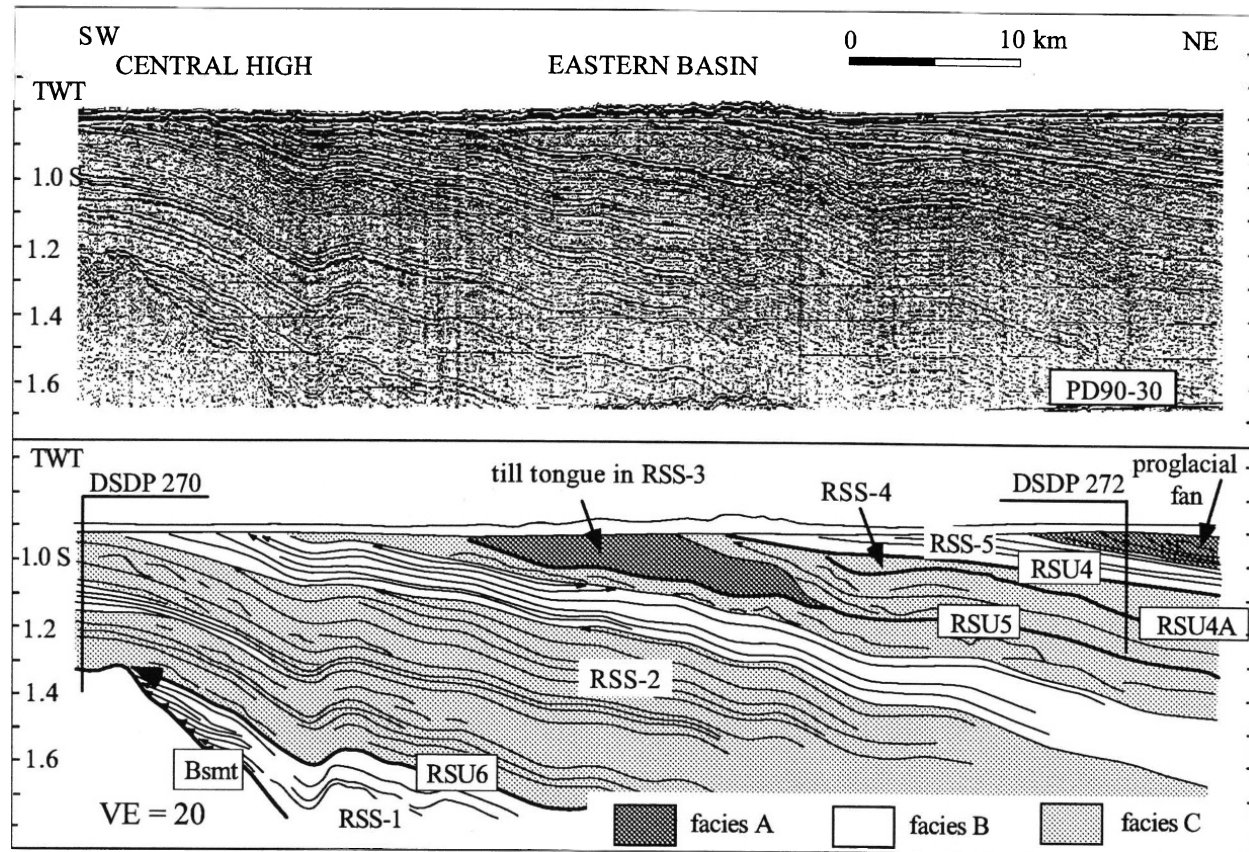


Fig. 9. Segment of seismic profile PD90-30 (intermediate-resolution data) and interpretation. This line shows seismic facies C and B of RSS-2 crossing DSDP Site 270 and facies C of RSS-3 and RSS-4 crossing DSDP Site 272. A facies A feature, interpreted by [Anderson and Bartek, 1992] as a till tongue, occurs in RSS-3 within a facies C unit. Note that RSU6 onlaps onto the basement flank. Folds in RSS-1 and RSS-2 are less evident in RSS-3 and RSS-4 and are absent above RSU4. See Figure 6 for profile location.

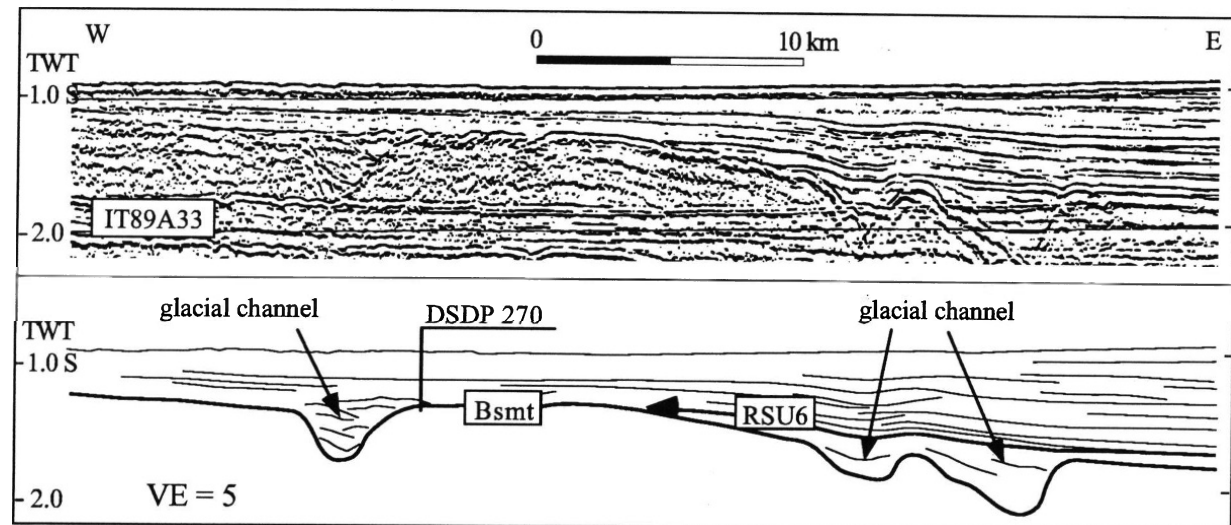


Fig. 10. Segment of seismic profile IT89A-33 (low-resolution data) and interpretation. This profile shows that U-shaped channels cut into acoustic basement. We interpret these as glacial channels. See Figure 11c for profile location.

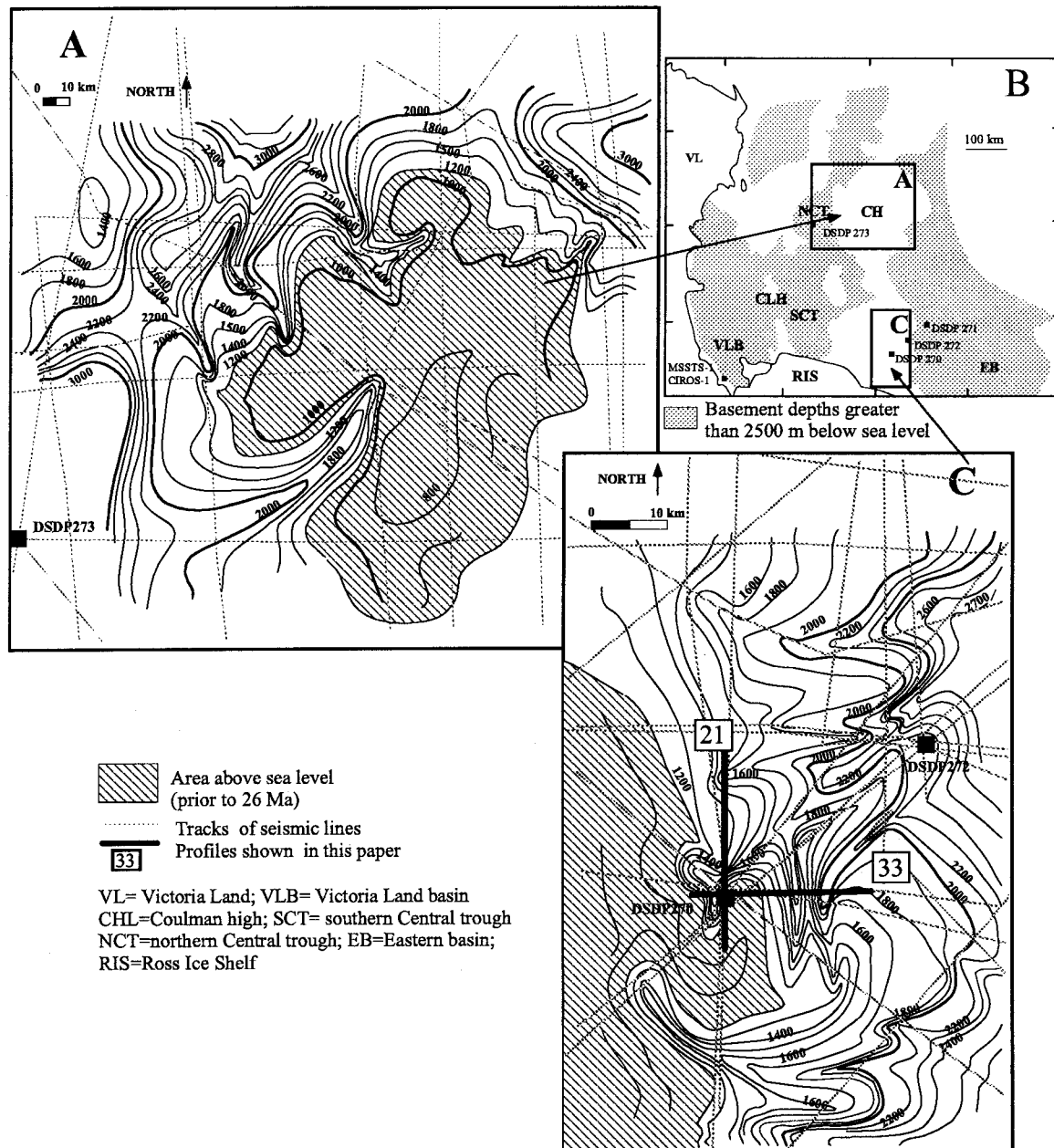


Fig. 11. Structural maps of the acoustic basement. Depths are from sea surface to basement in two-way travel time). a) north sector of Central high and c) south sector of the Central high. Numbers in squares correspond to the seismic sections shown in this paper: 33 = IT89A33, Figure 10; 21 = PD90-21, Figure 8. b) Location map showing the outline of major sedimentary basins.

also in the Eastern basin near the shelf break at RSU3 time (Figure 14). These surfaces are also similar in scale to the bathymetric troughs on the Ross Sea continental shelf today, and they too extend to the continental shelf break.

4.2. Seismic Facies

Deposits of RSS-1 were not sampled at DSDP sites, so their lithologic nature can only be inferred from

their seismic character. This stratified seismic facies fills the deepest parts of the continental shelf basins, as observed in MCS data, and represents the gradual deposition of likely non-marine and marine sequences since rifting of the Ross Sea [Cooper *et al.*, 1991b].

RSS-1 lies mostly below the sea-floor multiple, which does not allow high- and intermediate-resolution single-channel seismic data sets to be used for seismic facies analysis.

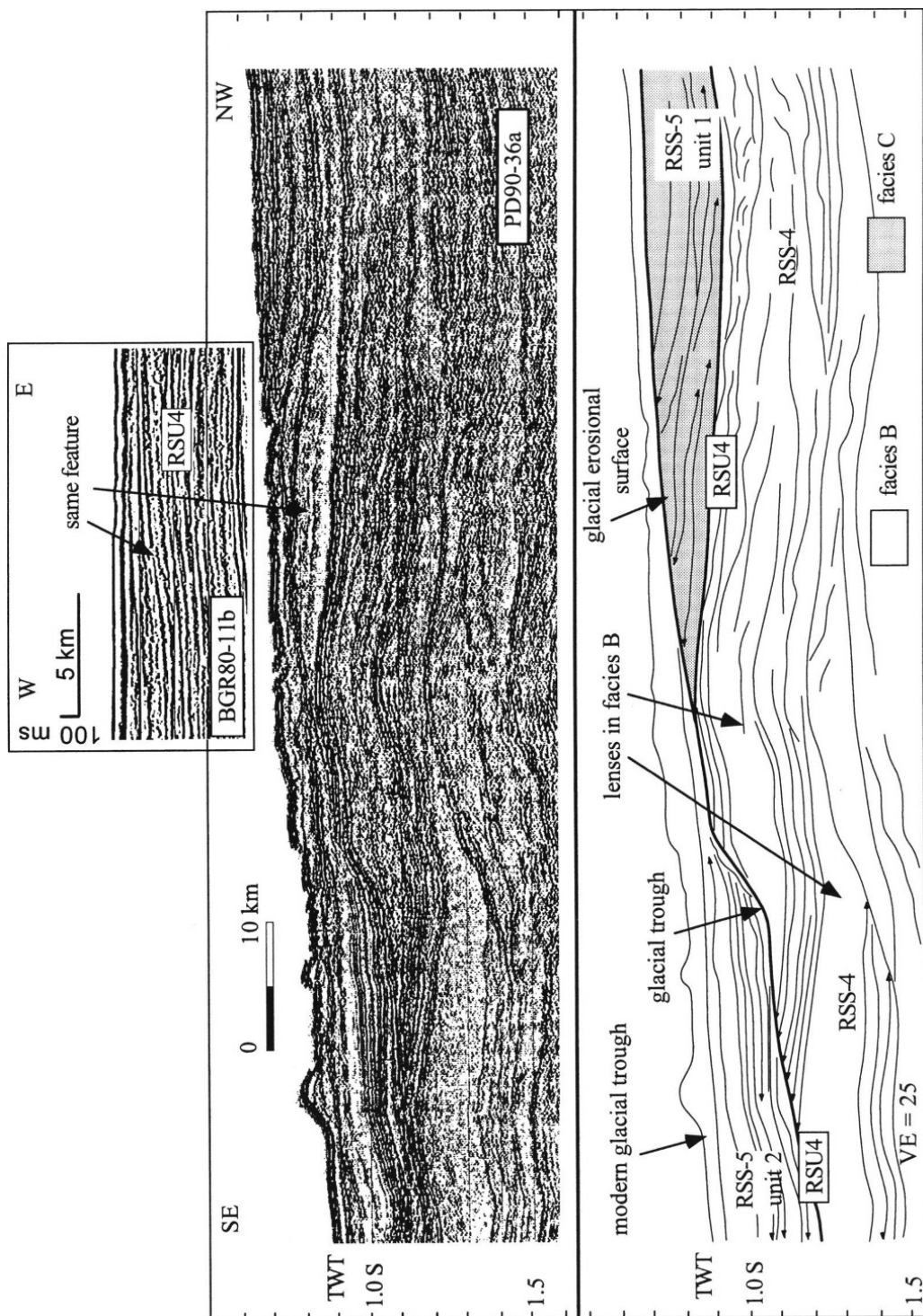


Fig. 12. Segment of seismic profile PD90-36a (intermediate-resolution data) and interpretation. The large glacial trough cut into RSS-4 is filled with facies B and C. We interpret these facies as glacial-marine deposits and gravity-flows respectively. Note the wedge of facies C on the western flank of a topographic high. This wedge is cut by an erosional surface that joins with RSU4 toward the southeast. A parallel low-resolution segment of profile BGR80-11b across the same feature is also shown. This profile shows the same wedge of facies C seen on line PD90-36a. See Figures 7 and 17 for profile locations.

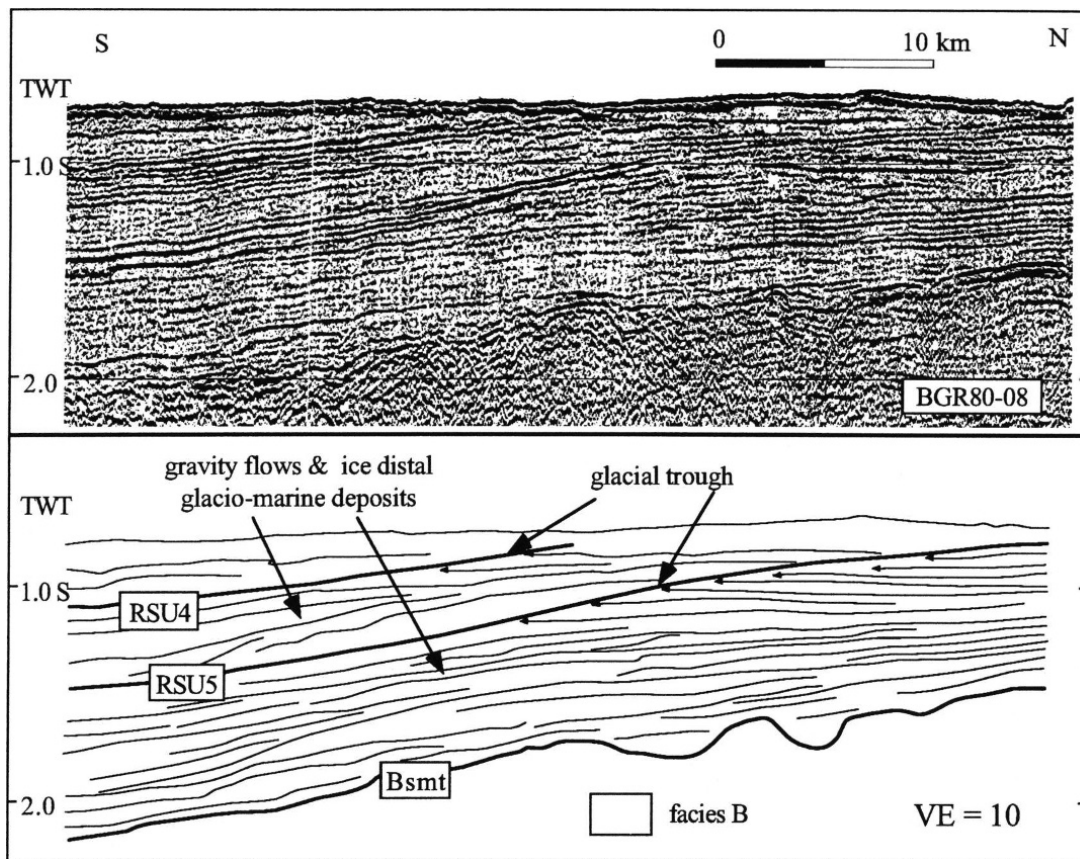


Fig. 13. Segment of seismic profile BGR80-08 (low-resolution data) and interpretation illustrating one flank of each of two large erosional troughs cut by RSU4 and RSU5. See Figure 7 for profile location.

The massive facies A deposits within sequences RSS-2 through RSS-5 are mostly observed over the structural highs. Seismic facies A was sampled in RSS-5 at DSDP Site 272 (Figures 2a and 15). This facies corresponds to a stratigraphic interval that consists of pebbly mudstone, and is interpreted by *Hambrey and Barrett* [1993] as compound glacial-marine rocks interbedded with diamictites. Diamictites are interpreted by *Balshaw* [1981] as ice-proximal deposits. We think that these strata indicate that the grounding line of the ice sheet was fluctuating close to the site. Hence, we believe facies A formed by progradation and lateral migration of proglacial deposits [*Powell*, 1990, 1991; *Powell and Molnia*, 1989; *Boulton*, 1990, *Anderson and Bartek*, 1992; *Hambrey*, 1994].

The well-stratified seismic facies B that occurs in all the sequences, from RSS-1 to RSS-5, is the most widespread and common facies on the continental shelf, and has a maximum thickness of about 6–8 km.

Sedimentary rocks that correspond to seismic facies B within RSS-2 were sampled at DSDP Site 270 (Figures 8 and 15) and consist of finely and coarsely stratified silty claystone with rare and small clasts [*Hayes and Frakes*, 1975]. These deposits were interpreted by *Hambrey and Barrett* [1993] as having been deposited in a variable ice-proximal to ice-distal environment. Ice-raftered debris (IRD) concentrations in these deposits are less than those in deposits that correspond to facies C at the same site. The combined seismic and lithologic characteristics of facies B suggest to us a less turbid glacial setting, relative to facies A and C, as might be expected in an ice-distal environment. The lithofacies associated with facies B within RSS-4 at DSDP Site 273 (Figures 16 and 15) consists of diatomaceous pebbly silty claystone [*Hayes and Frakes*, 1975], and are interpreted by *Hambrey and Barrett* [1993] as mainly compound glacial-marine sediments that were deposited in an ice-distal setting.

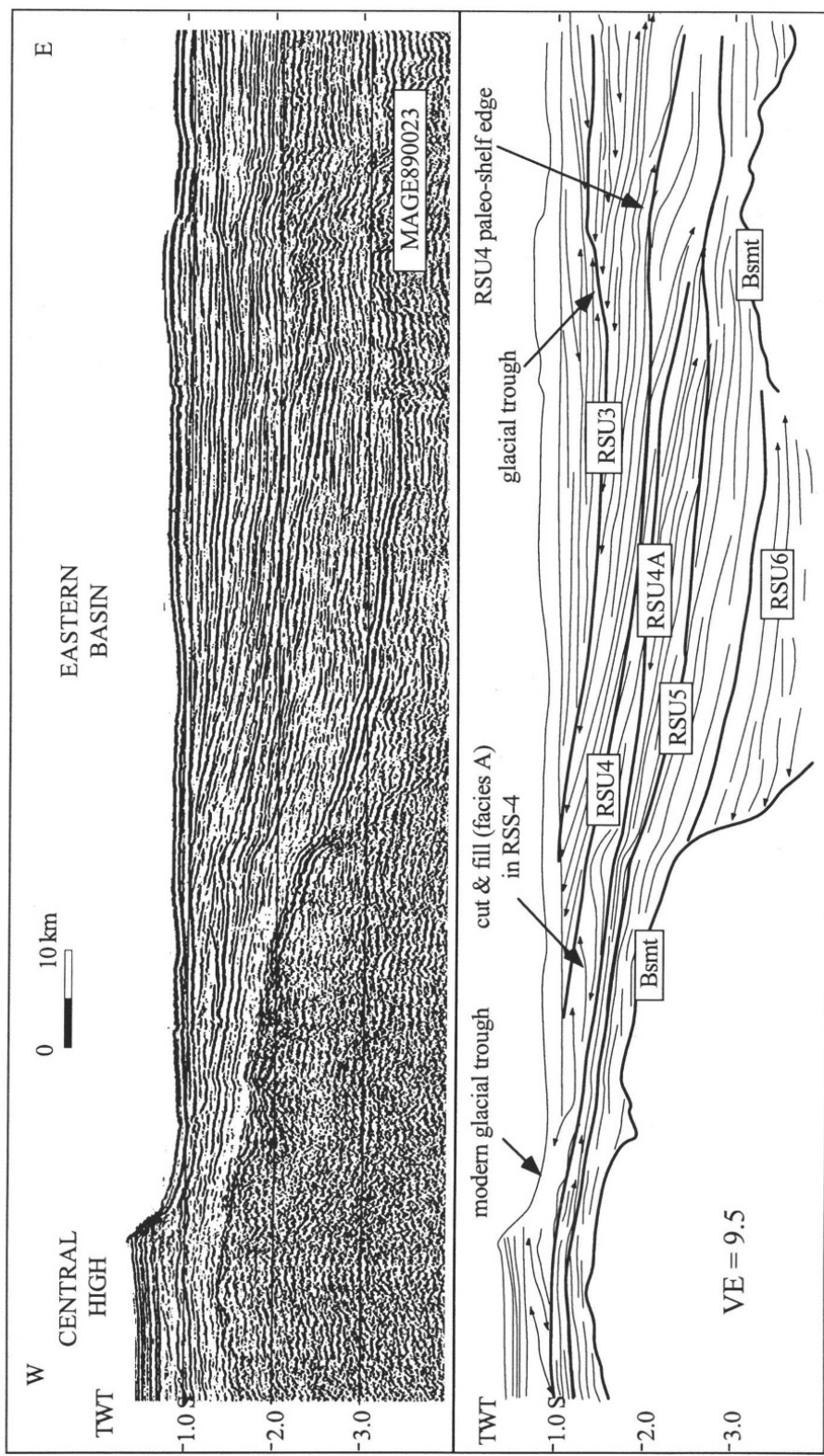


Fig. 14. Segment of seismic profile MAGE890023 (low-resolution data) and interpretation. Note the large trough cut by RSU3 and filled by stratified facies and prograding units from the east. In the Eastern basin, sequence boundaries older than RSU3 are low-angle erosional surfaces, nearly concordant with overlying and underlying strata of facies B. See Figure 6, 7, 17, 18 for profile location.

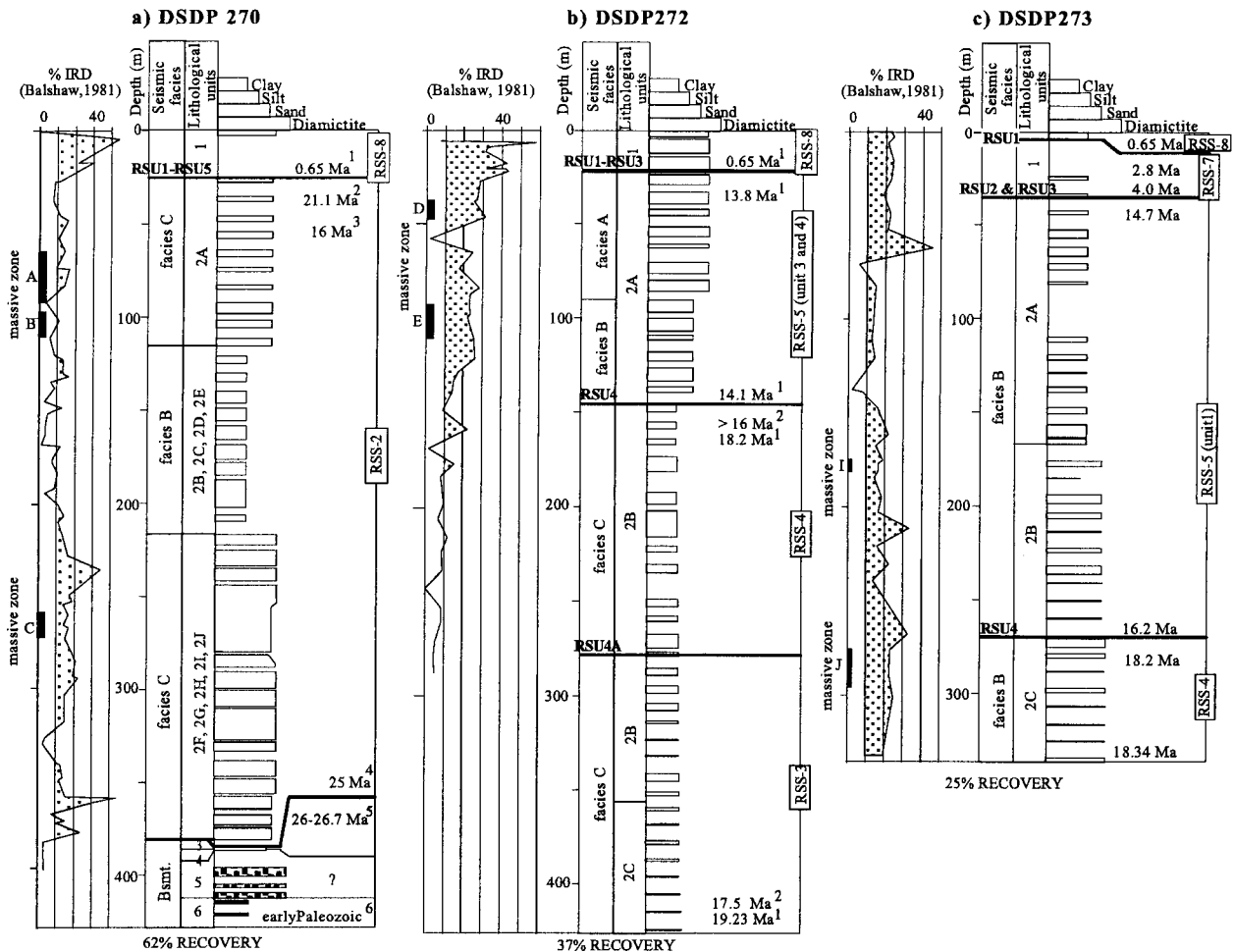


Fig. 15. Descriptions for DSDP Sites 270, 272 and 273 in the Ross Sea. (a) Site 270 ages are from: 1 = Hayes and Frakes [1975], 2 = Steinhauff and Webb [1987], 3 = Allis et al. [1975], 4 = D'Agostino and Webb [1980], Leckie and Webb [1986], 5 = McDougall [1977], and 6 = Ford and Barrett [1975]. (b) Site 272 ages are from: 1 = Savage and Ciesielski [1983] and 2 = Leckie and Webb [1986]. (c) Site 273 ages are from Savage and Ciesielski [1983]. Ice-raftered debris percentages (% IRD) and massive zones A through E are from Balshaw [1981]. Lithologic and biostratigraphic descriptions are from Hayes and Frakes [1975].

Some sediments, corresponding to facies B at DSDP site 273, were influenced by strong bottom currents and by rapid deposition from sediment-laden icebergs coming from glaciers in the Transantarctic Mountains [Balshaw, 1981, Barrett, 1975]. Small and thin-walled foraminifera occur in these deposits and indicate a less stressful, probably more ice-distal environment [D'Agostino and Webb, 1980]. We infer similar ice-distal depositional setting for facies B of RSS-5, based on silty claystones [Balshaw, 1981] that were sampled from this unit at DSDP Site 272 (Figure 15).

Scattered, massive lenses, draped by stratified units, are common in seismic facies B within RSS-2 and RSS-4 (Figure 12). We interpret these lenses as sediment gravity-flows deposited in an ice-distal environment because (1) the lenses grade into a generally subhorizontal, stratified facies, and (2) the lenses occur in basinal areas separated by several km from massive ice-proximal facies (A and C) at the same stratigraphic level. The large thickness of facies B and relatively high sedimentation rates for cored deposits [450 m/Ma at Site 272, Savage and Ciesielski, 1983], implies to us

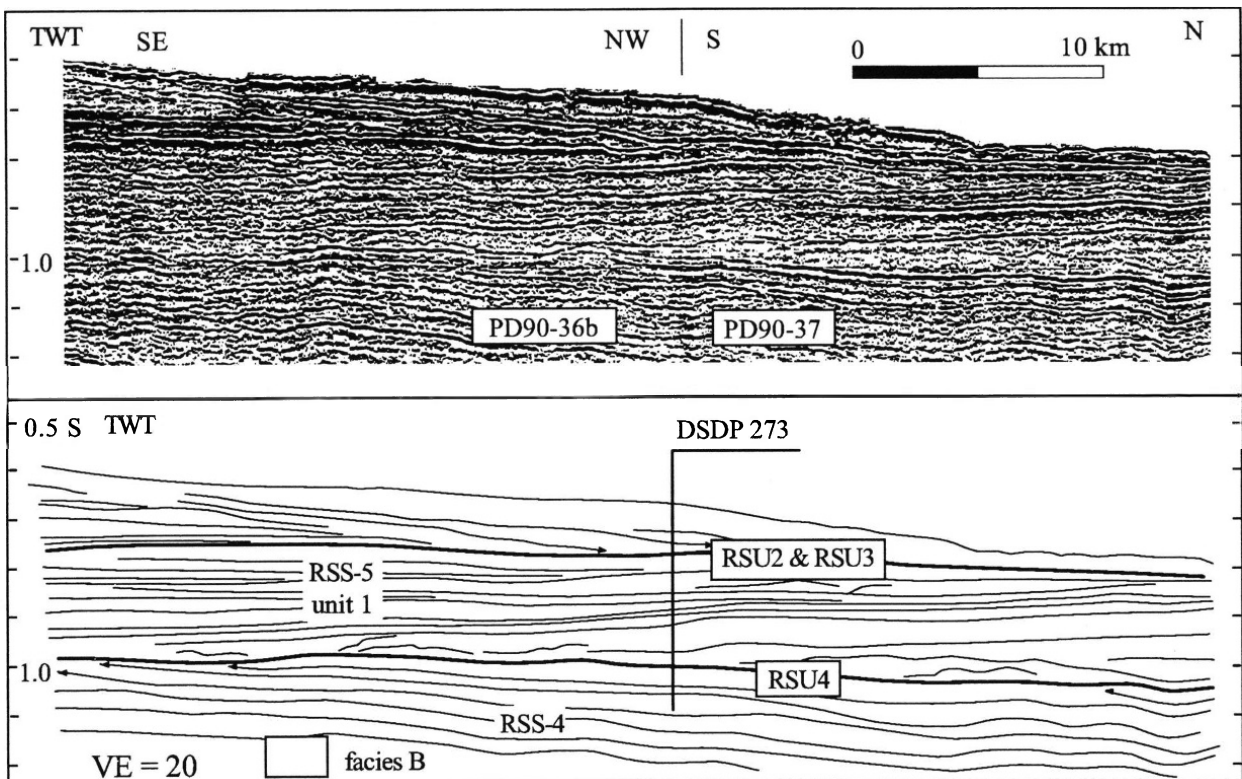


Fig. 16. Segment of seismic profile PD90-36b and PD90-37 (intermediate-resolution data) and interpretation. This profile shows stratified seismic facies B in RSS-4 and RSS-5 extending through DSDP Site 273. The partly reflective lens above RSU4 is interpreted by us as either a gravity-flow deposit or grounding-line proximal deposit. See Figure 7 for profile location.

melt-water sedimentation. Facies B also filled deep glacial troughs that were carved across the Central high within RSS-3, RSS-4 (Figure 13) and RSS-5 (Figure 12).

Seismic facies C within RSS-2 consists of massive and coarsely stratified silty-claystone that was sampled at DSDP Site 270 (Figures 8 and 15). These rocks were interpreted by *Hambrey and Barrett* [1993] as lodgment till and waterlain till. *Balshaw* [1981] identified "massive zones" in DSDP Site 270 cores and interpreted them as transitional glacial-marine deposits. In both cases, an ice-proximal setting is implied. *Anderson and Bartek* [1992] interpreted this seismic facies as including till tongues deposited on subglacial erosion surfaces. The fan-like geometry of this facies perhaps indicates that these are grounding-line fans. Dip lines across the Eastern basin show that massive to chaotic lenses of facies C were deposited in RSS-4 on paleo-slopes ($1\text{--}2^{\circ}$), and were draped by a stratified facies (Figure 9). In these settings, we believe facies C

may be gravity-flow deposits interbedded with glacial-marine sediments. Facies C in RSS-4 was sampled at DSDP Site 272 (Figures 9 and 15) and corresponds to diatom silty claystone and silty clay diatomite with rare clasts [*Hayes and Frakes*, 1975]. This lithofacies was interpreted by *Balshaw* [1981] and *Hambrey and Barrett* [1993] as an ice-distal glacial-marine facies. The sedimentation rate within facies C at DSDP Site 272 is 275 m/Ma [*Savage and Ciesielski*, 1983], which is much lower than the sedimentation rate of coeval, more ice-distal facies B at DSDP Site 273 [450 m/Ma, *Savage and Ciesielski*, 1983]. The higher rates near the basin center (Site 273) may be due to sediment bypassing the sloping basin flanks (e.g., Site 272) to reach the basin centers (e.g., Site 273). *Hayes and Frakes* [1975] note evidence at Site 272 for transport and deformation of sediment in facies C during deposition.

In summary, we interpret facies A as grounding zone proximal deposits that likely accumulated as

prograding fans with associated sediment gravity-flows. Our interpretations are consistent with those of *Anderson and Bartek* [1992]. We interpret facies B as an ice-distal glacial-marine facies that fills basins on the shelf. We believe that facies C is an ice-proximal facies that is probably composed of gravity-flows draped by glacial-marine sediments, generally deposited seaward of facies A.

INTERPRETED LATE OLIGOCENE AND MIOCENE GLACIAL HISTORY OF THE ROSS SEA CONTINENTAL SHELF

The late Oligocene and Miocene glacial history of the Ross Sea has been partly controlled by morphology of acoustic basement. The depth contour map of acoustic basement (*ANTOSTRAT*, this volume, Plate 19d) shows that the Ross Sea has several basins, separated by basement highs, that formed mostly since Cretaceous time (Figure 11b; *Cooper et al.*, 1991b). Other depth-contour maps for unconformities in the overlying sedimentary section (e.g. RSU6, RSU4A and RSU4; Figures 6, 7 and 17), although not corrected for sediment compaction and subsidence, in conjunction with isopach maps for sequences RSS-2 to RSS-5 [*ANTOSTRAT*, this volume, Plates 20-22], give a general idea of the possible paleo-morphology of the continental shelf at these times. These maps show that buried basins and highs are present now, and we believe they likely existed during the deposition of the late Oligocene and Miocene sequences (RSS-2 to RSS-5, Table 2). Basement beneath the main structural highs (Central and Column highs) was locally exposed above the onlap points for RSU6 (Figure 6). These basement features remained as bathymetric highs at least until middle Miocene time (see depth contour map of RSU4A, Figure 7). Moreover, the depth contour map of RSU4A shows that the Central trough comprised a narrow set of segmented depocenters, and the Eastern basin was a broad crustal sag (Figure 7). A wide, east-west oriented structural valley (about 100 km wide) separated the northern and southern Central high since RSS-1 time, and was deeply eroded at RSU5 (Figure 13) and RSU4 times (Figures 12 and 13).

In the western Ross Sea, CIROS-1 recovered middle Eocene and early Oligocene sediments, with a glacial component, within the upper part of RSS-1 [*Brancolini et al.*, this volume(b)]. There are no age constraints for RSS-1 in the central and eastern Ross Sea, but it is interpreted to be Oligocene or older in age (*Busetti and*

Cooper, 1994) because it lies below subaerial and shallow-water deposits at the base of DSDP Site 270 dated by *McDougal* [1977] as older than 26-26.7 Ma. We suggest that prior to late Oligocene-early Miocene time, the shallowest areas of the continental shelf were exposed, and temperate outlet glaciers probably carved the U-shaped channels observed on these basement highs. RSU6, which is the downlap surface separating RSS-2 early Miocene glacial-marine units (Figure 8) from the sediments of RSS-1 that fill the channels, may be a sequence boundary that formed during the 30 Ma sea-level low stand of *Haq et al.* [1987].

Glacial erosion at about 30 Ma that we postulate from seismic data may be associated with the relative maximum in average ice volume inferred for the Oligocene at 29-32 Ma [*Keigwin and Keller*, 1984]. During transgression, which coincided with a eustatic rise between 30 and about 25 Ma [*Haq et al.*, 1987], these glaciers retreated, the channels were filled with interglacial sediments and marine sands that were deposited over a terrestrial paleosol at DSDP Site 270. The boundary between non-glacial glauconitic sandstone [*Hayes and Frakes*, 1975] and glacial-marine rocks at DSDP Site 270 (within RSS-2) is an erosional surface, possibly a glacial unconformity [*Anderson and Bartek*, 1992]. Above this unconformity, sediments of DSDP Site 270 record a gradual increase in water depth, from 100 to 300 m [*Leckie and Webb*, 1983], and a transition from ice-proximal glacial-marine (facies C) to more ice-distal glacial-marine sediments (facies B) (Figure 8). In the same stratigraphic interval, terrestrially-derived biogenic material decreases upwards in the section [*Hayes and Frakes*, 1975]. Spores and pollen indicate the presence of coastal vegetation and, therefore, a temperate climate [*Kemp*, 1975], although still glacial [*Hayes and Frakes*, 1975].

Near DSDP site 270, the deposition of ice-proximal facies C (in RSS-2) above ice-distal facies B (Figure 8), indicates to us renewed intensification of glacial conditions during the same period that *Leckie and Webb* [1983] established that water depths in this area were increasing from 300 to 500 m. *Anderson and Bartek* [1992] suggest that the increase in water depth recorded by microfossils in the basal glacial-marine strata of DSDP Site 270 was due to subglacial erosion by a grounded ice sheet. They argued that subglacial erosion best explains the absence of transitional sediments. Tectonic activity before RSU4 is indicated by subtle folding of strata below RSU4, shown in seismic lines near DSDP 270 (Figure 9). We infer that

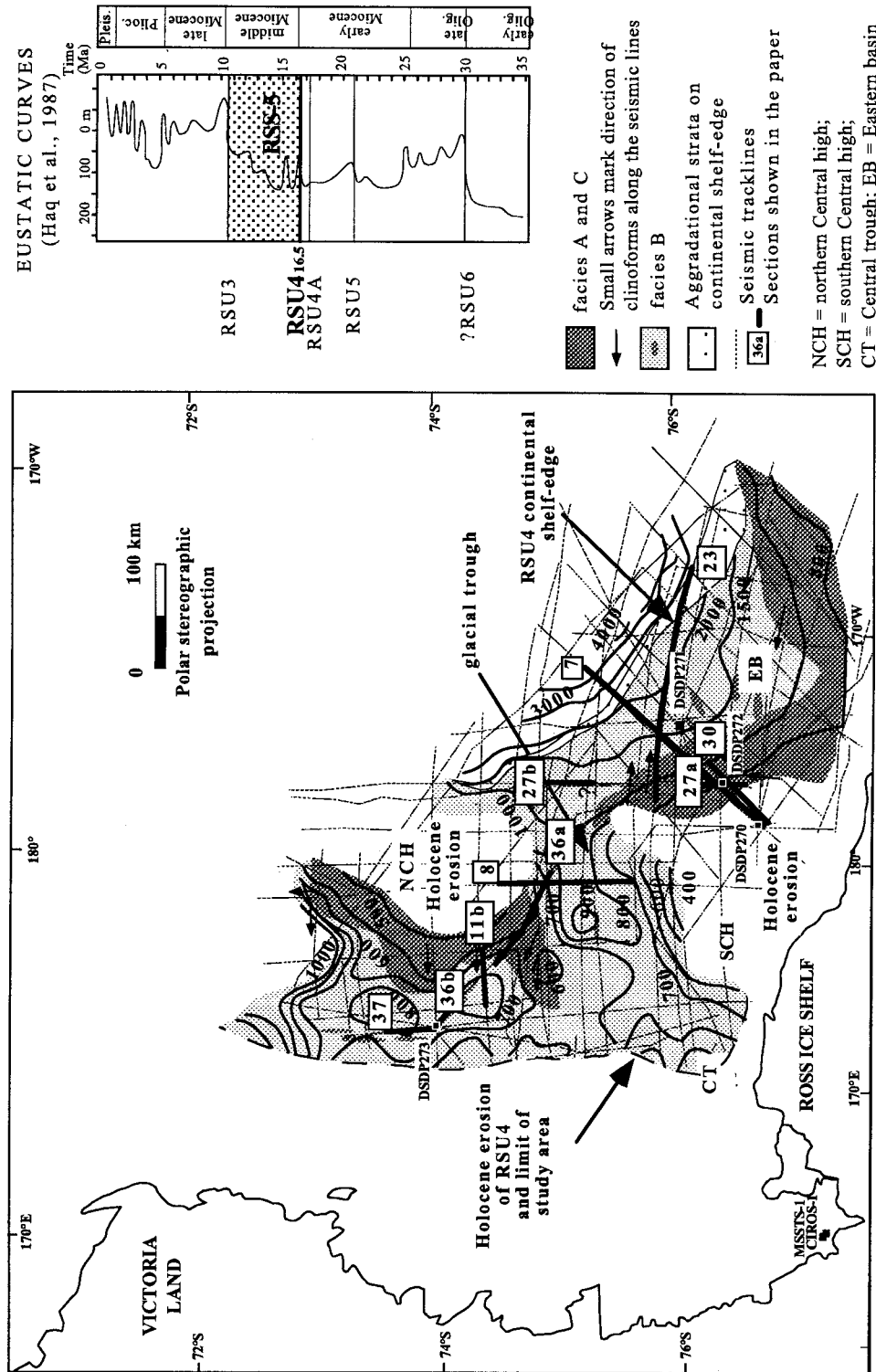


Fig. 17. Structural contour map of RSU4 (depths below sea surface in meters) and distribution of seismic facies in the lower middle Miocene sequence RS5-5. Numbers in squares correspond to the seismic sections shown in this paper: 27a = MAGE890027 section a, Figure 2a; 27b = MAGE890027 section b, Figure 2b; 7 = BGR80-07, Figure 7; 30 = PD90-30, Figure 9; 36a = PD90-36 section a, Figure 12; 11b = BGR80-11 section b, Figure 12; 8 = BGR80-08, Figure 13; 23 = MAGE890023, Figure 14; 36b = PD9036 section b, Figure 16; 37 = PD90-37, Figure 16.

fast tectonic subsidence, coupled with frequent episodes of glacial erosion, may have caused the observed water depth increase and associated increase in accommodation space. Overall, the inferred tectonic subsidence within RSS-2, between 26 Ma [McDougal, 1977] and 21.2 Ma [Steinrauf and Webb, 1987], increased paleowater depth from 50 to 500 m at DSDP Site 270 [Leckie and Webb, 1983].

The strata deposited on the structural highs around DSDP site 270 during this time interval exhibit vertical alternations of at least three facies: a massive facies C (ice-proximal), a more stratified facies B (ice-distal), and again a more massive facies C (Figure 8). We interpret the alternating facies as resulting from transgressive/regressive cycles (facies C/B and B/C), and the erosion of the surfaces that bound these cycles as being caused by ice volume and eustatic changes. Similar vertically alternating seismic facies A (ice-proximal), facies B (ice-distal) and facies A (ice-proximal) are observed in younger sequences, RSS-2 to RSS-4 (Figure 4). A further example is seen on the Central high, where massive facies A (ice-proximal) is cut by RSU4 and is overlain by a thick layer of facies B in RSS-5 (ice-distal) and then covered by a massive facies A (Figure 9).

Seismic sections show that RSU5 occurs between the top of DSDP Site 270 and the bottom of DSDP Site 272 (Figure 9). The age of RSU5 is, therefore, still uncertain. RSU4A was drilled at DSDP Site 272 in sediments dated as 18.2-19.2 Ma by *Savage and Ciesielski* [1985] and as about 16-17.5 Ma by *Leckie and Webb* [1986]. If we assume that RSU5 and RSU4A are equivalent to low-latitude eustatic sequence boundaries as defined by *Haq et al.* [1987] and as having been formed during sea-level falls, as suggested also by their truncation at the shelf edge (Figure 3), then we can equate RSU5 and RSU4A to sea level falls at 21 and 17.5 Ma respectively. In this scenario, the large proglacial delta-like features observed in RSS-3 and RSS-4, above these unconformities, may have formed during sea-level low stand intervals. At this time, local ice caps on the basement highs on the central shelf advanced to the edge of surrounding basins, where the ice caps deposited large proglacial deltas, like those seen in facies A (Figures 2a, 3, 4). Where the grounding line was situated near a steep slope (e.g. the eastern flank of the Central high in the Eastern basin), sediments were transported downslope by sediment gravity flow processes and were covered by glacial-marine sediments (Figure 9).

Prograding wedges of facies A, cut by erosion surfaces like RSU5, RSU4A and RSU4 (Figure 2a), suggest to us gradual advance of ice caps onto shallow areas of the continental shelf. The deposition of ice-distal facies B above subglacial erosional surfaces, such as RSU4 (Figure 4) on the inner shelf near the structural highs, implies (a) retreat of the ice caps toward shallower areas of the continental shelf and (b) lateral migration or backstepping of proglacial deposits, perhaps during a marine transgression.

Cooper et al. [1991a], *Anderson and Bartek* [1992] and *Cochrane et al.* [1994] favor a subglacial origin for most of the Miocene sequence boundaries of the Ross Sea. In the basins that surround the basement highs, the older (late Oligocene-early Miocene) sequence boundaries are low angle truncation surfaces, typically without large erosional relief (e.g., troughs) (Figures 3 and 14). The minimal erosion would argue against a subglacial origin for the late Oligocene-early Miocene sequence boundaries on the outer continental shelf.

At Site 272, RSU4 has an age of 14.2 Ma (i.e., age of overlying sediments) and a hiatus of about 4 Ma [*Savage and Ciesielski*, 1983] (Figure 15). RSU4 results from the amalgamation of several unconformities in the vicinity of Site 272. In the expanded section of DSDP Site 273, close to the center of the Central trough, RSU4 is concordant with younger and older strata. Here, RSU4 is younger than 16.2 Ma and has a hiatus of about 2 Ma [*Savage and Ciesielski*, 1983] (Figure 15). When RSU4 was formed, possibly coincident with the 16.5 Ma sea-level low stand of *Haq et al.* [1987], local ice caps may have expanded onto the continental shelf. However, there is no seismic evidence that ice was grounded at DSDP Site 273 at this time. The conformable geometry of RSU4 here (Figure 16) indicates that it was perhaps formed by marine erosion, rather than glacial erosion. Sparse bedding and sandy lags at approximately the level of RSU4 in DSDP Site 273 have been interpreted as hiatuses caused by bottom currents [*Savage and Ciesielski*, 1983], probably because these sand layers lie between relatively deep-water glacial-marine sediments. However, there is no sedimentary or fossil evidence to indicate water depth at the time RSU4 was eroded, and therefore a shallow water origin cannot be excluded [*Barrett, personal communication*, 1995]. Lithofacies transitional between shallow and deep-water sediments are missing above RSU4, but the absence could be due to the poor recovery at DSDP Site 273.

We believe that an ice sheet advanced and retreated across the Central high during the late early-Miocene. There are several lines of evidence.

1. A proglacial feature occurs in the lower part of RSS-5 on the western flank of the Central high, and is cut by an erosional surface that amalgamates with RSU4 toward the southeast (Figure 12). Here (at DSDP Site 273), RSS-5 is from 16.2 to 14.7 Ma.

2. A large (hundreds of km) glacial trough (Figures 12 and 13) lies between the northern and southern Central high, and is filled with ice-distal sediments (unit 2 of RSS-5) that are apparently younger than the proglacial fan in unit 1 of RSS-5 (Figure 12).

3. The sedimentary section younger than 14.2 Ma [Savage and Ciesielski, 1983], is marked by ice-distal seismic facies (facies B) and lithofacies (DSDP Site 272) in RSS-5 (Figure 2a).

Thinning, decoupling and retreat of a middle Miocene ice sheet from banks on the central part of the Ross Sea continental shelf may have been partly in response to a temperature maximum noted by Prentice and Matthews [1988] at 15.5 to 15.0 Ma, and to a widespread flooding event at 15 Ma [Haq *et al.*, 1987]. We suspect that the ice sheet again advanced and moved across ice-proximal facies A (in the upper part of RSS-5) and across ice-distal facies B (Figure 2a) within the Eastern basin, between 14.2 and 13.8 Ma [Savage and Ciesielski, 1983]. The colder climates that we infer from seismic facies in RSS-5 are consistent with colder global climate and assumed Antarctic ice growth between 16 and 13.5 Ma derived from the Oxygen and Carbon isotope records [Shackleton and Kennett, 1975; Savin *et al.*, 1981; Woodruff *et al.*, 1981; Prentice and Matthews, 1988].

By RSU3 time, ice sheets were carving troughs on the central and eastern Ross Sea continental shelf. The seismic data (Figure 14) and the depth contour map of RSU3 (Figure 18) show the first occurrence of a broad glacial trough in the Eastern basin. This trough trends SSW-NNE. We believe that RSU3 resulted from subglacial erosion, although the extent of glacial advance at RSU3 time cannot be determined because the western flank of the glacial trough has been uplifted and eroded (Figure 14). The age(s) of RSU3 event(s) are also uncertain because RSU3 is commonly amalgamated with other unconformities, and these are large hiatuses (13 Ma at DSDP site 272; about 10 Ma at DSDP site 273; Savage and Ciesielski [1983]). In the interval 4.0 to 13.8 Ma the Haq *et al.* [1987] eustatic sea-level curve shows a gradual regressive trend that ends with a large sea level fall at 10 Ma. We suspect

that the 10 Ma low stand coincided with increased ice volumes and a maximum ice-sheet expansion onto the Ross Sea continental shelf.

Ice sheets grounded on the eastern parts of the continental shelf in the late Miocene and Pliocene, as evidenced by the ice-proximal seismic facies and associated glacial unconformities that are dominant features there in RSS-6, RSS-7 and RSS-8. Climates may have been more temperate than today during the deposition of RSS-5 to at least RSS-7, as noted also by Alonso *et al.* [1992] who report possible troughs, due to melt-water subglacial streams, in Pliocene sedimentary units. A large thickness of stratified facies with high accumulation rates also characterize RSS-5, suggesting to us that melt-water may have played a more important sedimentological role than at present. Similar relationships are seen in other melt-water environments [Anderson and Ashley, 1991].

Late Pleistocene sequences are characterized by massive lenses and a paucity of laminated packages [Shipp *et al.*, 1994], suggesting that truly polar conditions may have been established in the eastern sector of the Ross Sea by Plio-Pleistocene time. Similar findings are reported for the western Ross Sea by Brancolini *et al.* [this volume(b)].

CONCLUSIONS

Our interpretation of glacial and glacial-marine seismic facies and erosional surfaces in seismic reflection profiles with different resolutions led to a reconstruction of the late Oligocene-late Miocene glacial history of the central and eastern Ross Sea. Correlation with DSDP drill site data provided age and lithologic control for the seismic facies interpretation. High- to intermediate-resolution seismic data were used to characterize seismic facies and to identify most glacial erosion surfaces on the shelf. Low-resolution seismic data were used for regional correlation of large-scale acoustic facies and sequence boundaries.

Facies character and distribution patterns in the late Oligocene to middle Miocene section imply that temperate glacial conditions existed, and that depositional processes were related to the presence of local ice caps centered near banks in the middle of the Ross Sea. Our scenario for glaciation on the continental shelf during the late Oligocene is consistent with the evidence for Oligocene glaciations in Marie Byrd Land [LeMasurier and Rex, 1982] and in the western Ross Sea [Barrett, 1986; 1989; Hambrey *et al.*, 1989].

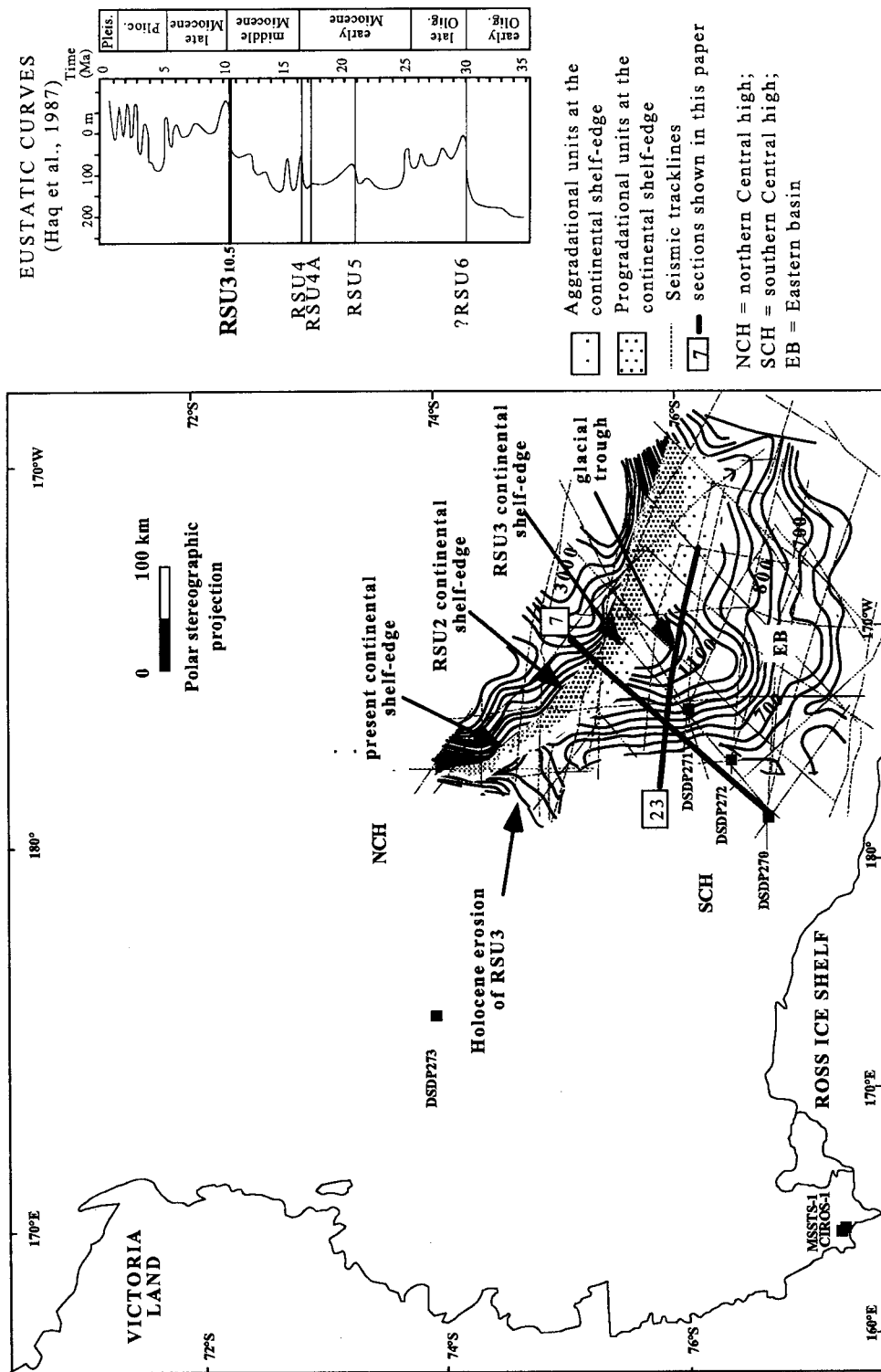


Fig. 18. Structural contour map of RSU3 (depths below sea surface in meters). Numbers in squares correspond to the seismic sections shown in this paper: 7 = BGR80-07, Figure 3; 23 = MAGE890023, Figure 14.

Tectonic activity throughout the Ross Sea [Cooper *et al.*, 1994] perhaps elevated areas where ice caps developed. In the early Miocene during eustatic sea-level low stands, ice caps developed on, and across banks of the central Ross Sea. In the Eastern basin, sediment supply was not great enough to keep pace with tectonic subsidence. Consequently, ice caps flowing from the Central high, and possibly from Marie Byrd Land, were not able to construct a shallow proglacial platform over which to advance into the deeper basinal areas of the shelf. Once tectonic subsidence slowed after middle to late Miocene time, basins were filled by glacial-marine sediments, creating shallower platforms on which ice caps could ground onto the outer shelf.

Large-scale growth of ice caps occurred during the time that RSS-5 was deposited (middle-to-late Miocene between about 16.5 and perhaps 10 Ma) and ended with widespread erosion (RSU3) that we interpret to coincide with the development of a temperate to sub-polar ice sheet.

In the eastern Ross Sea, the first evidence of a grounded polar ice-sheet across the eastern Basin exists in the late Miocene-early Pliocene section (sequence RSS-6 and RSS-7). At that time

1. Large glacial troughs were carved on the outermost sector of the Eastern basin.
2. Widespread ice proximal seismic facies were deposited on the continental shelf in the eastern Basin.
3. Topset beds of outer-shelf sediment wedges, with steep foresets, were deeply cut by glacial erosion surfaces at the shelf edge.

Acknowledgments. We would like to thank K. Hinz and the Bundesanstalt für Geowissenschaften und Rohstoffe, Germany; A. Cooper and the United States Geological Survey; J. Wannesson and the Institut Français du Pétrole; S. Sato and the Japanese National Oil Company; the Joint Stock Marine Arctic Geological Expedition, Russia; the U.S. National Science Foundation; and the Osservatorio Geofisico Sperimentale, Italy, for kindly providing access to the seismic data used in this investigation. We also thank H. Josenhans, L. Bartek, P. Carlson, and P. Barrett for helpful reviews of the paper. A. Cooper provided useful editorial assistance, for which we are grateful. M. Busetti participated in the interpretation of the MCS data, identification of sequences boundaries, and the compilation of depth contour maps. This work was funded by University of Parma (Italy), under grant of Doctorate of Research with Prof. Luigi Torelli.

REFERENCES

- Allis, R. G., P. J. Barrett, and D. A. Christoffel, A paleomagnetic stratigraphy for Oligocene and early Miocene marine glacial sediments at site 270, Ross Sea, Antarctica, in *Initial Reports of the Deep Sea Drilling Project*, vol. 28, pp. 879-884, U.S. Government Printing Office, Washington D.C., 1975.
- Alonso, B., J. B. Anderson, J. I. Diaz, and L. R. Bartek, Pliocene-Pleistocene seismic stratigraphy of the Ross Sea: evidence for multiple ice sheet grounding episodes, in *Contribution to Antarctic Research III. Antarctic Research Series*, vol. 57, edited by D. H. Elliot, pp. 93-103, AGU, Washington, D. C., 1992.
- Anderson, J. B., and G. M. Ashley (eds.), Glacial marine sedimentation; paleoclimatic significance, *Geological Society of America, Special Paper 261*, 232 pp., 1991.
- Anderson, J. B., and L. R. Bartek, Cenozoic glacial history of the Ross Sea revealed by intermediate resolution seismic reflection data combined with drill site information, in *The Antarctic Paleoenvironment: a Perspective on Global Change. Antarctic Research Series*, vol. 56, edited by J. P. Kennett and D. A. Warnke, pp. 231-263, AGU, Washington, D. C., 1992.
- ANTOSTRAT Project, Seismic Stratigraphic Atlas of the Ross Sea, Antarctica, this volume.
- Armentrout, J. M., Glacial lithofacies in the Neogene Yakataga Formation, Robinson Mountains, Southern Alaska Coast Range, Alaska, in *Glacial Marine Sedimentation*, edited by B. F. Molnia, pp. 629-666, Plenum Press, New York, 1983.
- Armentrout, J. M., Application of sequence stratigraphy in glaciated terrain: examples from Gulf of Alaska Neogene outcrops and seismic reflection profiles, *Terra Antarctica*, 1(2), 419-420, 1994.
- Balshaw, K. M., Antarctic glacial chronology reflected in the Oligocene through Pliocene sedimentary section in the Ross Sea, Ph.D. thesis, Rice University, Houston, Texas, 140 pp., 1981.
- Barrett, P. J., Textural characteristic of Cenozoic preglacial and glacial sediments at site 270, Ross Sea, Antarctica, *Initial Report, Deep Sea Drilling Project*, vol. 28, pp. 757-767, U.S. Government Printing Office, Washington D.C., 1975.
- Barrett, P. J., (Ed.), Antarctic Cenozoic history from MSSTS-1 drill hole, McMurdo Sound, *DSIR Bulletin 237*, Science Information Publishing Center, Wellington, 174 pp., 1986.
- Barrett, P. J., (Ed.), Antarctic Cenozoic history from CIROS-1 drill hole, McMurdo Sound, *DSIR Bulletin 245*, Science Information Publishing Center, Wellington, 254 pp., 1989.
- Bartek, L. R., L. C. Sloan, J. B. Anderson, and M. I. Ross., Evidence from the Antarctic Continental margin of late Paleogene ice sheets: a manifestation of plate reorganization and synchronous changes in atmospheric circulation over the emerging southern ocean?, in *Eocene-Oligocene Climatic and Biotic Evolution*, edited by D. R. Prothero and W. A. Berggren, pp. 131-159, Princeton Univ. Press, Princeton, New York, 1992;

- Belknap, D. F., R. C. Shipp, J. T. Kelley, and D. Schnitker, Depositional sequence modeling of late Quaternary geologic history, west-central Maine Coast, in *Studies in Maine Geology*, vol. 5, edited by R. D. Tucker and R. G. Marvinney, pp. 29-46, Augusta, Maine Geological Survey, 1989.
- Belknap, D. F. and R. C. Shipp, Seismic stratigraphy of glacial-marine units, Maine inner shelf, in *Glacial marine sedimentation; paleoclimatic significance*, *Geological Society of America, Special Paper 261*, edited by J. B. Anderson, and G. M. Ashley, pp. 137-158, 1991.
- Boulton, G. S., Sedimentary and sea level changes during glacial cycles and their control on glaciomarine facies architecture, in *Glaciomarine Environments: Processes and Sediments*, *Geological Society Special Publication*, vol. 53, edited by J. A. Dowdeswell and J. D. Scourse, pp. 15-52, London, 1990.
- Brancolini, G. et al., Descriptive text for the Seismic Stratigraphic Atlas of the Ross Sea, Antarctica, this volume(a).
- Brancolini, G., A. Cooper, and F. Coren, Seismic facies and glacial history in the western Ross Sea, Antarctica, this volume(b).
- Busetti, M. and A. K. Cooper, Possible ages and origins of unconformity U6 in the Ross Sea, Antarctica, *Terra Antarctica*, 1, (2), 341-344, 1994.
- Busetti, M. and I. Zayatz and Ross Sea Regional Working group, Distribution of seismic units in the Ross Sea, *Terra Antarctica*, 1, (2), 345-348, 1994.
- Carlson, P. R., T. R. Bruns, B. F. Molnia, and W. C. Schwab, Submarine valleys in the northeastern Gulf of Alaska: characteristic and probable origin, *Marine Geology*, 47, 217-242, 1982.
- Cochrane, G., L. De Santis and A. K. Cooper, Continuity of glacial sequences in the Ross Sea from sonobuoy seismic-refraction data, *Terra Antarctica*, 1, (2), 349-352, 1994.
- Cooper, A. K., P. J. Barrett, K. Hinz, V. Traube, G. Leitchenkov, and H. M. J. Stagg, Cenozoic prograding sequences of the Antarctic continental margin: a record of glacio-eustatic and tectonic events, *Marine Geology*, 102, 175-213, 1991a.
- Cooper, A. K., F. J. Davey, and K. Hinz, Crustal extension and origin of sedimentary basin beneath the Ross Sea and Ross Ice Shelf, Antarctica, in: *Geological Evolution of Antarctica*, edited by M. R. A. Thompson, J. A. Crame and J. W. Thompson, pp. 285-291, Cambridge University Press, Cambridge, 1991b.
- Cooper, A. K., G. Brancolini, J. C. Behrendt, F. J. Davey, P. J. Barrett, and ANTOSTRAT Ross Sea regional working group, A record of Cenozoic tectonism throughout the Ross Sea and possible controls on the glacial record, *Terra Antarctica* 1(2), 353-355, 1994.
- D'Agostino, A. and P. N. Webb, Interpretation of mid-Miocene to Recent lithostratigraphy and biostratigraphy at DSDP site 273, Ross Sea, *Antarctic Journal of the U.S.*, 15(5), 118-120, 1980.
- Ford, A. B. and P.J. Barrett, Basement rocks of the south-central Ross Sea, Site 270, DSDP Leg 28, in *Initial Reports of the Deep Sea Drilling Project*, vol. 28, pp. 861-868, U.S. Government Printing Office, Washington D.C., 1975.
- Hambrey, J. M. (Ed.), *Glacial Environments*, 296 pp., University College of London Press, London, 1994.
- Hambrey, M. J. and Barrett P. J., Cenozoic sedimentary and climatic record, Ross Sea region, Antarctica, in *The Antarctic Paleoenvironment: A Perspective on Global Change, Part 2*, edited by J. P. Kennett and D. A. Warnke, Antarctic Research Series, AGU, 60, pp. 91-124, Washington, D.C., 1993.
- Hambrey, M. J., P. J. Barrett, and P. H. Robinson, Stratigraphy, in *Antarctic Cenozoic History from the CIROS-1 Drill Hole, McMurdo Sound*, edited by P. J. Barrett, pp. 23-48, DSIR Bulletin 245, Wellington, 1989.
- Hannah, M. J., Eocene dinoflagellates from the CIROS-1 drill hole, McMurdo Sound, Antarctica, *Terra Antarctica*, 1(2), 371-372, 1994.
- Haq, B. U., J. Hardenbol, and P. R. Vail, The chronology of fluctuating sea level since the Triassic, *Science*, 235, 1156-1167, 1987.
- Hayes, D. E. and L. A. Frakes, *Initial Reports of the Deep Sea Drilling Project*, vol. 28, 1017 pp., U. S. Government Printing Office, Washington, D. C., 1975.
- Hinz, K., and M. Block, Results of geophysical investigations in the Weddell Sea and in the Ross Sea, Antarctica, in *Proceedings 11th World Petrol. Congress, London, 1983*, pp. 279-291, Wiley, New York, 1984.
- Houtz, R. E. and R. Meijer, Structure of the Ross Sea shelf from profiler data, *J. Geophys. Res.* 78, 6592-6597, 1970.
- Houtz, R. E. and F. J. Davey, Seismic profiler and sonobuoy measurements in the Ross Sea, Antarctica, *J. Geophys. Res.*, 78, 3448-3468, 1973.
- Jiang, X. and D. M. Harwood, A glimpse of early Miocene Antarctic forests: palynomorphs from RISP diatomite, *Antarctic Journal of the U.S.*, 27 (5), 3-6, 1992.
- Keigwin, L. D. Jr. and G. Keller, Middle Oligocene cooling from equatorial Pacific DSDP Site 77B, *Geology*, 12, 16-19, 1984.
- Kemp, E.M., Paleontology of Leg 28 drillsites, Deep Sea Drilling Project, in *Initial Reports of the Deep Sea Drilling Project*, vol. 28, pp. 599-608, U.S. Government Printing Office, Washington, D.C., 1975.
- King, L. H., Till in the marine environment, *Journal of Quaternary Science*, 8, (4), 347-358, 1993.
- King, L. H. and G. Fader, Wisconsinan glaciation of the continental shelf, southeast Atlantic Canada, *Bulletin Geological survey of Canada*, 363, 1-72, 1986.
- King, L. A., K. Rokoengen, G. Fader, and T. Gunleiksrud, Till-tongue stratigraphy, *Geological Society of America Bulletin*, 103, 637-659, 1991.
- Leckie, R. M. and P. N. Webb, Late Oligocene-early Miocene glacial record of the Ross Sea, Antarctica: evidence from DSDP Site 270, *Geology*, 11, 578-582, 1983.

- Leckie, R. M., and P. N. Webb, Late Paleogene and early Neogene foraminifera of Deep Sea Drilling Project Site 270, Ross Sea, Antarctica, in *Initial Reports of the Deep Sea Drilling Project*, vol. 90, pp. 1093-1142, U. S. Government Printing Office, Washington, D. C., 1986.
- LeMasurier, W. E. and D. C. Rex, Volcanic record of Cenozoic glacial history in Marie Byrd Land and Western Ellsworth Land: revised chronology and evaluation of tectonic factors, in *Antarctic Geoscience*, edited by C. Craddock, pp. 725-734, University of Wisconsin Press, Madison, 1982.
- McDougall, I., Potassium-Argon dating of glauconite from a greensand drilled at Site 270 in the Ross Sea, DSDP Leg 28, in *Initial Reports of the Deep Sea Drilling Project* vol. 36, pp. 1071-1072, U.S. Government Printing Office, Washington, D.C., 1977.
- Powell, R. D., Glacimarine processes at grounding-line fans and their growth to ice-contact deltas, in *Glacimarine Environments: Processes and Sediments*, pp. 53-73, Geological Society Special Publication of London, 53, 1990.
- Powell, R. D., Grounding-line systems as second-order controls on fluctuation of tidewater termini of temperate glaciers, in glacial marine sedimentation; paleoclimatic significance, *Geological Society of America, Special Paper 261*, edited by J. B. Anderson and G. M. Ashley, pp. 75-93, 1991.
- Powell, R. D. and B. F. Molnia, Glacimarine sedimentary processes, facies and morphology of the southeast Alaska shelf and fjords, *Marine Geology*, 85, 359-390, 1989.
- Prentice, M. L. and R. K. Matthews, Cenozoic ice-volume history: development of a composite oxygen isotope record, *Geology* 16 (11), 963-966, 1988.
- Saettem, J., D. A. R. Poole, L. Ellingsen, and H. P. Serjrup, Glacial geology of outer Bjoroyrenna, southwestern Barents Sea, *Marine Geology*, 103, 15-51, 1992.
- Savage, M. L. and P. F. Ciesielski, A revised history of glacial sediments in the Ross Sea region, in *Antarctic Earth Science*, edited by R. L. Oliver, P. R. James and J. B. Jago, pp. 555-559, Australian Academy of Science, Canberra, 1983.
- Savin, S. M., R. G. Douglas, G. Keller, J.S. Killingley, L. Shaughnessy, M.A. Sommer E. Vincent, and F. Woodruff, Miocene benthic foraminiferal isotope records: a synthesis, *Marine Micropaleontology*, 6, 423-450, 1981.
- Shackleton, N. J. and J. P. Kennett, Paleotemperature history of the Cenozoic and the initiation of Antarctic glaciation: oxygen and carbon isotope analyses in DSDP site 277, 279 and 281. DSDP Site 284, in *Initial Reports of the Deep Sea Drilling Project*, vol. 29, pp. 743-755, U.S. Government Printing Office, Washington, D.C., 1975.
- Shipp, R. C., D. F. Belknap, and J. T. Kelley, A submerged shoreline on the inner shelf off the Maine coast, northwestern Gulf of Maine, in *Studies in Maine Geology*, vol. 5, edited by R. D. Tucker, and R. G. Marvinney, pp. 11-28, Augusta, Maine Geological Survey, 1989.
- Shipp, S., J. B. Anderson, L. De Santis, L. R. Bartek, B. Alonso and I. Zayatz, High to intermediate-resolution seismic stratigraphic analysis of mid-late-Miocene to Pleistocene strata in eastern Ross Sea: implications for changing glacial/climatic regime, *Terra Antarctica*, 1 (2), 381-384, 1994.
- Steinhauff, D. M. and P. N. Webb, Miocene foraminifera from DSDP Site 270, Ross Sea, *Antarctic Journal of the U.S.*, 22(5), 125-126, 1987.
- Stocker, M.S., Glacially-influenced sedimentation on the Hebridean slope, northwest United Kingdom continental margin, in *Glacimarine Environments: Processes and Sediments*, edited by J. A. Dowdeswell and J. D. Scourse, pp. 349-362, Geological Society Special Publication of London, 53, 1990.
- Syvitski, J. P. M. Towards an understanding of sediment deposition on glaciated continental shelves, *Continental Shelf Research*, 11, 8-10, 897-937, 1991.
- Vorren, T. O., E. Lebesbye and K. B. Larsen, Geometry and genesis of the glaciogenic sediments in the southern Barents Sea, in *Glacimarine Environments: Processes and Sediments*, edited by J. A. Dowdeswell and J. D. Scourse, pp. 269-288, Geological Society Special Publication of London, 53, 1990.
- Woodruff, F., S. M. Savin and R. G. Douglas, Miocene stable isotope record: a detailed deep Pacific Ocean study and its paleoclimatic implications, *Science* 212, 665-668, 1981.
- J.B. Anderson, Department of Geology and Geophysics MS-126, Rice University, 6100 South Main St., Houston, Texas 77005-1892. G. Brancolini and L. De Santis Osservatorio Geofisico Sperimentale, PO Box 2011, 34016 Opicina (Trieste) Italy. I. Zayatz, Joint Stock Marine Arctic Geological Expedition, 26 Perovskaya St., Murmansk, 183012, Russia.

(Received February 15, 1995;
August 8, 1995)